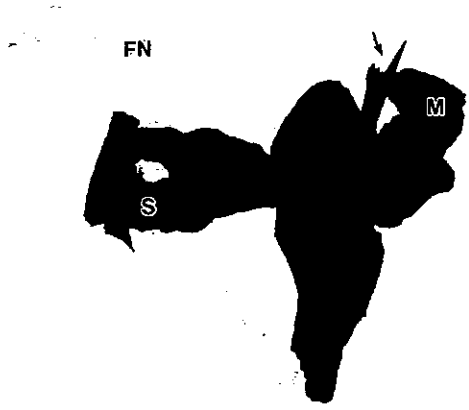

図5　耳小骨および顔面神経の三次元再構築像
ツチ骨（M）前突起が長く（矢印）、アブミ骨後脚が太い（S）。顔面神経（FN）は膝部の角度が鈍角である。

は1例のみである。すなわちThompsonら[3]は3例の小児について報告し、このうち2例には聴力検査で異常はなく、他の1例には聴力検査は行われていないが、言語機能から難聴はないものと思われる。松永ら[1]の37歳女性症例は聴性脳幹反応で正常所見を示していた。一方、Adachiら[4]は感音難聴を認めた5歳男児を報告しているが、難聴の程度など詳細な記載はされていない。

18p−症候群の側頭骨病理に関しては、これまで1例の報告もなされておらず、今回の自験例が初めて症例と思われる。本症例の側頭骨病理の主な異常所見は、耳小骨、顔面神経および蝸牛に見られた。耳小骨については、ツチ骨およびアブミ骨に異常がみられたが、耳小骨の発達については、胎生15週から20週で成人と同等のサイズと形態に成長するといわれていることから[6]、本症例の耳小骨の形態は明らかな異常と考えられる。顔面神経については、神経は細く、膝神経節細胞は減少し、神経の低形成を示していた。また神経膝部の角度は胎生16週までに直角になるといわれているが[7]本症例では鈍角走行を示し、さらに顔面神経管は水平部から垂直部にかけて大きく欠損し、異常形態を示していた。蝸牛については、その発達は胎生21週までに成人と同じ回転数とサイズになるため[6]、在胎24週の本症例の蝸牛は明らかに短蝸牛を示しているといえる。

以上のように、1）18p−症候群の報告例は比較的多いものの、18p−症候群の難聴に関しては、これまでその報告が殆ど見られていない。2）また本症例は身体的に重篤な奇形を有しているにもかかわらず、聴器病変は比較的軽度であった。これらのことから、18p−症候群は、他の重篤な染色体異常症候群と比較して、聴器障害が合併しにくいのが特徴ではないかと思われる。しかしいずれにしてもこの結論については、今後の症例の蓄積を待つしかないであろう。

まとめ

18p−症候群1例の側頭骨病理所見について報告した。本症例は18p−症候群の側頭骨病理所見を観察した最初の症例であると思われ、主に耳小骨、顔面神経、蝸牛に形態異常がみられた。しかし身体的に重篤な奇形を有しているにもかかわらず、聴器病変は比較的軽度であることから、本症候群には聴器障害は伴いにくいのが特徴ではないかと思われるが、この結論については今後の症例の蓄積を待つしかないであろう。

参考文献

1）松永　薫、久保雅寛、辻　貞俊、他：慢性多発筋炎を合併した第18番染色体短腕欠損症候群の1例．臨床神経学 33：980−984, 1993.
2）Fischer P, Golob E, Friedrich F, et al.：Autosomal deletion syndrome. —46, XX, 18p-：A new case report with absence of IgA in serum—. J Med Genet 7：91−98, 1970.
3）Thompson RW, Peters JE, Smith SD：Intellectual, behavioral, and linguistic characteristics of three children with 18p-syndrome. JDBP 7：1−7, 1986.
4）Adachi K, Hayashi M：An 18p- syndrome due to 15/18 translocation with facial palsy and deafness. Tohoku J Exp Med 133：307−311, 1981.
5）Shuknecht HF：Techniques for study of cochlear function and pathology in experimental animals. Arch Otolaryngol 58：377−397, 1953.
6）Nemzek WR, Brodie HA, Chong BW, et al.：Imaging findings of the developing temporal bone in fetal specimens. AJNR 17：1467−1477, 1996.
7）Declau F, Jacob W, Montoro S, et al.：Dehiscence of the facial canal：developmental aspects. Int J Pediatr Otorhinolaryngol 21：21−32, 1991.

論文受付　16年8月5日
論文受理　16年10月18日

別刷請求先：〒973−8403　いわき市内郷綴町沼尻3
福島労災病院耳鼻咽喉科　大谷　　巌

JOURNAL OF VIROLOGY, June 2004, p. 6282–6286 Vol. 78, No. 12
0022-538X/04/$08.00+0 DOI: 10.1128/JVI.78.12.6282–6286.2004

Induction of Suppressor of Cytokine Signaling-3 by Herpes Simplex Virus Type 1 Contributes to Inhibition of the Interferon Signaling Pathway

Shin-ichi Yokota,[1] Noriko Yokosawa,[1] Tamaki Okabayashi,[1] Tatsuo Suzutani,[2] Shunsuke Miura,[3] Kowichi Jimbow,[3] and Nobuhiro Fujii[1]*

Department of Microbiology[1] and Department of Dermatology,[3] Sapporo Medical University School of Medicine, Chuo-ku, Sapporo 060-8556, and Department of Microbiology, Fukushima Medical University School of Medicine, Fukushima 960-1295,[2] Japan

Received 26 November 2003/Accepted 5 February 2004

We showed previously that herpes simplex virus type 1 (HSV-1) suppresses the interferon (IFN) signaling pathway during the early infection stage in the human amnion cell line FL. HSV-1 inhibits the IFN-induced phosphorylation of Janus kinases (JAK) in infected FL cells. In the present study, we showed that the suppressor of cytokine signaling-3 (SOCS3), a host negative regulator of the JAK/STAT pathway, is rapidly induced in FL cells after HSV-1 infection. Maximal levels of SOCS3 protein were detected at around 1 to 2 h after infection. This is consistent with the occurrence of HSV-1-mediated inhibition of IFN-induced JAK phosphorylation. The HSV-1 wild-type strain VR3 induced SOCS3 more efficiently than did mutants that are defective in UL41 or UL13 and that are hyperresponsive to IFN. Induction of the IRF-7 protein and transcriptional activation of IFN-α4, which occur in a JAK/STAT pathway-dependent manner, were poorly induced by VR3 but efficiently induced by the mutant viruses. In contrast, phosphorylation of IRF-3 and transcriptional activation of IFN-β, which are JAK/STAT pathway-independent process, were equally well induced by the wild-type strain and the mutants. In conclusion, the SOCS3 protein appears to be mainly responsible for the suppression of IFN signaling and IFN production that occurs during HSV-1 infection.

Cells have various defense mechanisms that protect them from viral infection. In turn, viruses suppress or escape host responses by a variety of strategies. Interferon (IFN) is induced by viral infection and plays an important role in the defense of the host cell from viral attack. When IFN binds to specific cell surface receptors on the host cells, it promotes the antiviral state through induction or activation of the 2′,5′-oligoadenylate synthetase (2-5AS)/RNase L system, the double-stranded RNA-activated protein kinase, and the MxA protein (10, 30, 35). The signal transduction pathway of IFN consists of Janus kinases (JAK), tyrosine protein kinases that interact with the intracellular domains of the receptors, and the STAT family proteins, transcription factors that are activated by their phosphorylation by JAK. This pathway, which is designated the JAK/STAT pathway, also transduces various cytokine signals. There are four JAK proteins (Jak1, Jak2, Jak3, and Tyk2) and seven STAT proteins (STAT1 to 4, STAT5a, STAT5b, and STAT6) (1, 9, 17, 25). Each cytokine employs a particular combination of the JAK and STAT proteins, which determines the specificity of the cytokine responses. For instance, Jak1 and Tyk2 are associated with the IFN-α/β receptor complex. These JAK proteins are activated by phosphorylation after IFN-α/β binds to the receptor, and they then phosphorylate STAT1 and STAT2. The transcription factor ISGF3, which consists of phosphorylated STAT1, phosphorylated STAT2, and IRF-9/p48/ISGF3γ, forms and then translocates into the nucleus and binds to IFN-stimulated response elements in the promoters of IFN-inducible genes (9, 12).

DNA and RNA viruses use various strategies to counteract the IFN-induced antiviral response (2, 11–13, 22). Blocking the JAK/STAT pathway, which is an entrance of IFN action, is a more efficient way to counteract the host defense reaction than inhibiting each of the IFN-induced effector molecules individually. It has been reported by Miller et al. (20, 21) that of the *Herpesviridae*, human cytomegalovirus downregulates the expression of Jak1 and IRF-9. Recently, we demonstrated that herpes simplex virus type 1 (HSV-1) suppresses IFN-induced JAK phosphorylation during the early infection stage in the human amnion cell line FL but not in the human monocytic cell line U937 (44). In the present study, we showed that HSV-1 induces a host inhibitor of the JAK/STAT pathway, specifically the suppressor of cytokine signaling-3 (SOCS3) protein. The SOCS family proteins are STAT-induced STAT inhibitors that constitute a negative feedback system of the JAK/STAT pathway. These proteins commonly share an N-terminal region of variable length, a central src homology 2 domain, and a C-terminal SOCS box. SOCS proteins are generally expressed at low levels in cells, and transcription of their genes is induced by various cytokines that activate the JAK/STAT pathway (3, 7, 14, 41). To date, eight SOCS family proteins (SOCS1 to 7 and CIS) have been identified. CIS, SOCS1, SOCS2, and SOCS3 have been reported to inhibit the signal transduction of various types of cytokines. Of these, SOCS1 and SOCS3 have been reported to inhibit the signal transduction of IFN (4, 36, 38).

* Corresponding author. Mailing address: Department of Microbiology, Sapporo Medical University School of Medicine, South-1, West-17, Chuo-ku, Sapporo 060-8556, Hokkaido, Japan. Phone: 81-11-611-2111. Fax: 81-11-612-5861. E-mail: fujii@sapmed.ac.jp.

MATERIALS AND METHODS

Cells and viruses. The human amnion cell line FL was routinely cultured in RPMI-1640 containing 10% fetal bovine serum. The HSV-1 strain VR3 was obtained from the American Type Culture Collection (Manassas, Va.). UL41-defective (d41) and UL13-defective (d13) mutants derived from VR3 were prepared as described previously (37, 39). Unless otherwise mentioned, virus infection was performed at a multiplicity of infection of 5 (MOI 5). Virus titers in the culture supernatant were determined by a plaque-forming assay using Vero cells as an indicator. Virus inactivation by UV irradiation was performed according to a previous report (44).

Plasmids and transient transfection. Human SOCS3 cDNA was prepared by reverse transcription-PCR (RT-PCR) using cellular RNA derived from FL cells infected with HSV-1 for 10 min as a template. The primer set for preparing full-length SOCS3 cDNA was as follows: sense, 5′-ATGGTCACCCACAGCA AGTT-3′; antisense, 5′-CTTAAAGCGGGGCATCGTACTG-3′. The resulting PCR product was ligated into a mammal expression vector, pTargeT vector (Promega, Madison, Wis.) and cloned.

The plasmid was transfected into cells by using SuperFect reagent (Qiagen, Hilden, Germany) according to the manufacturer's instruction manual. After 24 h of transfection, the cells were treated with human IFN-α (Serotec, Oxford, United Kingdom) at a final concentration of 1,000 IU/ml.

Western blotting. Preparation of total cell lysates, sodium dodecyl sulfate-polyacrylamide gel electrophoresis, and Western blotting were carried out as described previously (43, 44). Rabbit anti-SOCS3 antibody was purchased from IBL (Gunma, Japan). Rabbit anti-STAT1, anti-IRF-3, and anti-IRF-7 antibodies were purchased from Santa Cruz Biotechnology (Santa Cruz, Calif.). Rabbit anti-phospho-STAT1 (Tyr701) antibody was from Cell Signaling (Beverly, Mass.). Alkaline phosphatase-conjugated anti-rabbit or mouse immunoglobulin antibodies (BioSource, Camarillo, Calif.) and bromochloroindolylphosphate-nitroblue tetrazolium were used as secondary antibodies and the enzyme substrate for Western blotting, respectively. The resulting protein bands were scanned on a flatbed scanner and quantified by using the NIH Image program (National Institutes of Health, Bethesda, Md.).

RT-PCR. Total cellular RNA was prepared by using the RNeasy Mini kit (Qiagen). RT-PCR was performed with the OneStep RT-PCR kit (Qiagen). The quantitative nature of the PCR was validated by the linearity of the determination curve at various concentrations of RNA. The primer sets used to detect SOCS3, SOCS1, and CIS mRNA have been described elsewhere (29, 33). The primer sets used for IFN-β and IFN-α4 have been described previously (28). The following primer sets were used for 2-5AS: sense, 5′-CCAGGAAATTAGGAG ACAGC-3′; antisense, 5′-TGGCAGGGAGGAAGCAGGAG-3′. The primers for IRF-3 were the following: sense, 5′-GACCCTCACGACCCACATAA-3′; antisense, 5′-ACCCCACCAGCCGCAGGCCC-3′. The primers for IRF-7 were as follows: sense, 5′-GAGCCCTTACCTCCCCTGTTAT-3′; antisense, 5′-CCA CTGCAGCCCCTCATAG-3′. The primer set for actin was purchased from Clontech, and that for glyceraldehyde-3-phosphate dehydrogenase (GAPDH) has been described previously (42).

RESULTS

Suppression of the JAK/STAT pathway by HSV-1. In an earlier study, our group showed that HSV-1 suppresses the IFN-induced phosphorylation of JAK, STAT1, and STAT2 during the early infection stage in FL cells (44). In the present study, we further examined the effects on the JAK/STAT pathway of IFN-sensitive HSV-1 mutants that are defective in tegument proteins UL41 and UL13 (designated d41 and d13, respectively). These mutants display higher sensitivity to IFN compared to the wild-type strain, VR3 (37, 39). Figure 1 shows the effects of virus infection on IFN-α-induced STAT1 phosphorylation in FL cells. Infection (after 3 h) with the wild-type strain, VR3, almost completely suppressed IFN-α-induced STAT1 phosphorylation (Fig. 1A) and 2-5AS mRNA expression (Fig. 1B). This inhibition was observed after 2 h of infection and continued until cytopathic effects were observed (data not shown) (44). In contrast, infection with d41 and d13 only partially inhibited IFN-α-induced STAT1 phosphorylation and 2-5AS mRNA expression. Compared to the uninfected control, both responses were still nevertheless weaker and delayed by d41 or d13. d41 inhibited the IFN-α-induced responses more weakly than d13. These results indicate that the suppression of the JAK/STAT pathway by HSV-1 largely contributes to viral resistance to IFN and that the viral tegument proteins UL41 and UL13 take some part in this inhibition.

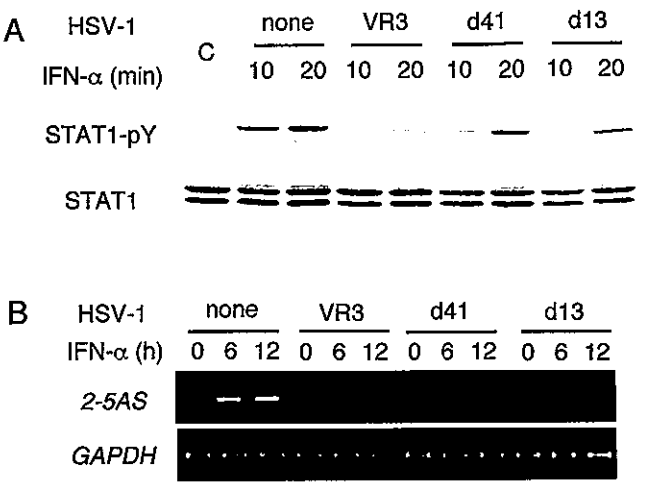

FIG. 1. Effects of infection with HSV-1 strain VR3, a UL41-deficient mutant (d41), or a UL13-deficient mutant (d13) on IFN-α-induced tyrosine phosphorylation of STAT1 (A) and induction of 2-5AS mRNA (B) in FL cells. FL cells were infected with HSV-1 VR3 or the d41 or d13 mutant at MOI 5 for 3 h. (A) The infected cells were treated with 1,000 IU of IFN-α/ml for 10 or 20 min. The cell lysates were then subjected to sodium dodecyl sulfate-polyacrylamide gel electrophoresis on a 7.5% polyacrylamide slab gel and analyzed by Western blotting using anti-STAT1 and anti-tyrosine phosphorylated STAT1 (STAT1-pY) antibodies. C, uninfected control. (B) The infected cells were treated with 1,000 IU of IFN-α/ml for 6 or 12 h, after which total cellular RNA was extracted. 2-5AS mRNA levels were determined by RT-PCR. GAPDH mRNA levels were determined as a control.

SOCS3 is induced by HSV-1. To reveal the mechanism by which HSV-1 inhibits the JAK/STAT pathway, we examined the expression of the SOCS family proteins. Western blot analysis showed that SOCS3 protein levels were markedly upregulated by HSV-1 infection after 1 to 2 h of VR3 infection (Fig. 2A and B). This time course is in agreement with that for the observed inhibition of IFN signaling (44). With regard to SOCS3 mRNA levels, they increased between 10 and 20 min after infection, and maximal levels were observed at 30 and 60 min (Fig. 3A). The mRNA levels rapidly decreased after 2 h of infection. For VR3 and d41, SOCS3 mRNA levels were slightly higher at 4 h than at 2 h postinfection. The reason for this is unclear, but it could be a secondary response. On the other hand, SOCS3 protein levels were maintained at similar levels, even at around 12 h after infection (Fig. 2C). The induction of SOCS3 protein and mRNA is dependent on the virus MOI (Fig. 2D and 3B). The d41 and d13 mutant viruses only weakly upregulated the inhibitor, SOCS3, at the levels of mRNA (Fig. 3C) and protein (Fig. 2B). The lower induction of SOCS3 by the tegument-deficient mutants compared to the wild-type strain was consistent with the weaker inhibition of IFN-α-induced JAK/STAT signaling (Fig. 1). When the wild-type virus, VR3, was inactivated by UV irradiation, it did not induce SOCS3 protein (Fig. 2C). SOCS1 and CIS were little or not

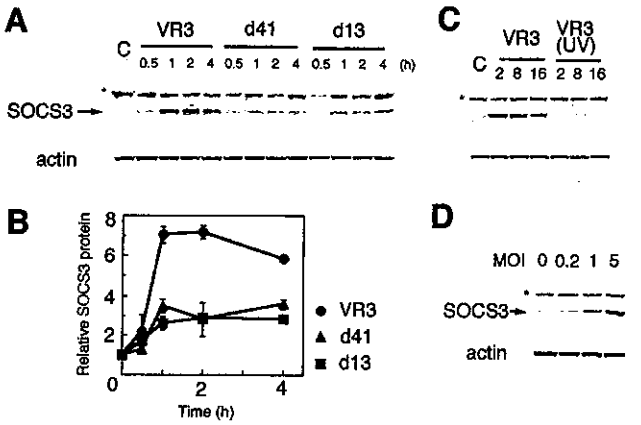

FIG. 2. Induction of SOCS3 protein by HSV-1 infection. (A and B) FL cells were infected with HSV-1 VR3 or the d41 or d13 mutant at MOI 5 for various periods. (A) The infected cell lysates were then analyzed by Western blotting using anti-SOCS3 antibody. Actin was employed as a control for protein loading. (B) Each band was quantified, and the results of the experiments performed in triplicate (means ± standard deviations) are shown. (C) FL cells were infected with HSV-1 VR3 or UV-inactivated virus for various periods. (D) FL cells were infected with VR3 at various MOIs for 2 h, and the levels of SOCS3 protein were then determined. The expression of SOCS3 protein was detected by Western blotting (arrow). *, nonspecific binding; C, uninfected control.

induced by HSV-1 and the mutants (Fig. 3C), which indicates that HSV-1 inhibits the JAK/STAT pathway by specifically inducing SOCS3.

IFN signal transduction is inhibited by overexpression of SOCS3. To assess whether SOCS3 can repress IFN-induced JAK/STAT signaling, we transiently overexpressed SOCS3 in FL cells by transfection with the pSOCS3 expression plasmid and then treated them with IFN-α. IFN-α-induced STAT1 phosphorylation was clearly suppressed in cells transfected with pSOCS3 (Fig. 4). These results indicate that HSV-1-induced SOCS3 is sufficient for the suppression of IFN signaling.

Suppression of the JAK/STAT pathway leads to inhibition of IRF-7 induction. We also characterized the effect of the virus-induced SOCS3 protein on the system that produces IFN. IFN production via the JAK/STAT pathway has been well characterized (5, 18, 31). Initially, IFN-β is transcriptionally activated

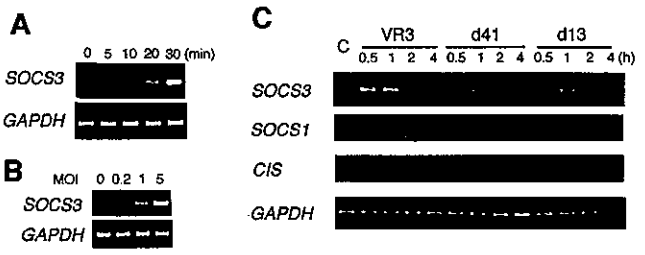

FIG. 3. Induction of SOCS3 mRNA by HSV-1 infection. (A) FL cells were infected with HSV-1 VR3 at MOI 5 for various periods. (B) FL cells were infected with VR3 at various MOIs for 30 min. The levels of SOCS3 mRNA were determined by semiquantitative RT-PCR. (C) FL cells were infected with HSV-1 VR3 or the d41 or d13 mutant at MOI 5 for various periods. The SOCS1, SOCS3, and CIS mRNA levels in the infected cells were analyzed by semiquantitative RT-PCR. GAPDH was determined as a control. C, uninfected control.

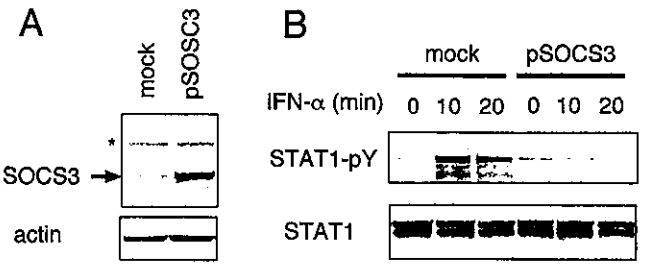

FIG. 4. Overexpression of SOCS3 suppresses IFN-α-induced Tyr-phosohorylation of STAT1. FL cells were transiently transfected with the SOCS3 expression plasmid (pSOCS3). (A) The expression of SOCS3 was determined by Western blotting. (B) After 24 h of transfection, the cells were treated with IFN-α (1,000 IU/ml) for 10 or 20 min. The cell lysates were then analyzed for the Tyr phosphorylation status of STAT1 by Western blotting. Actin and STAT1 were used as controls. *, nonspecific binding.

by phosphorylated IRF-3 and activated NF-κB. Both transcription factors are activated by various extracellular stimuli, including microorganisms and their components, in a JAK/STAT pathway-independent manner. We found that in FL cells challenged with VR3, d41, and d13, IRF-3 was equally well phosphorylated, as revealed by slower-migrating bands in Western blots compared to the unphosphorylated form (Fig. 5B). IFN-β mRNA induction was also upregulated to a similar extent by the three virus strains (Fig. 5A).

In general, virus-induced IFN-β stimulates the expression of

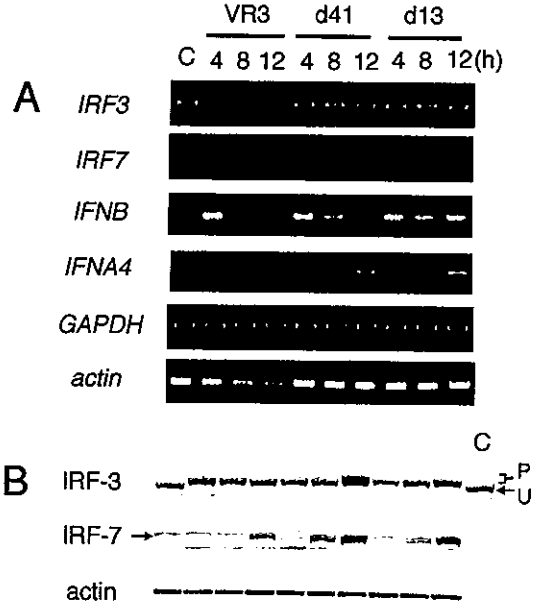

FIG. 5. Semiquantitative RT-PCR analysis of IRF-3, IRF-7, IFN-β, and IFN-α4 mRNA (A) and Western blotting analysis of IRF-3 and IRF-7 (B) in FL cells during infection with HSV-1 VR3 or the d41 or d13 tegument protein-deficient mutant. FL cells were infected with virus at MOI 5 for various periods. The phosphorylation status of IRF-3 was determined by Western blotting using an anti-IRF-3 antibody. Unphosphorylated and phosphorylated forms of IRF-3 are indicated by U and P, respectively. In contrast, total protein levels of IRF-7 are shown. C, uninfected control. Actin mRNA and protein (RT-PCR and Western blotting) and GAPDH mRNA (RT-PCR) were determined as controls.

IRF-7, a component of the transactivator of IFN-α genes, to produce large amounts of IFN, via the JAK/STAT pathway in an autocrine or a paracrine manner (5, 18, 31). In turn, IRF-7 mediates the induction of IFN-α and various IFN-inducible genes. In human cells, the expression of IFN-α4 is not activated but rather is inhibited by cooperative interactions between IRF-3 and NF-κB (32). Consequently, it appears that the induction of the IFN-α4 gene is IRF-7 dependent but not IRF-3 dependent. In other words, it is considered to be dependent upon the JAK/STAT pathway but not the IRF-3/NF-κB pathway. We found that infection of FL cells with the wild-type strain, VR3, poorly induced IRF-7 protein, even though IFN-β was induced (Fig. 5). However, the IRF-7 protein levels were increased by the two mutants defective in tegument proteins (Fig. 5B). These results indicate that the inhibition of the JAK/STAT pathway due to HSV-1 infection leads to significant blockage of JAK/STAT-dependent IFN production and to suppression of the antiviral effectors that are regulated by IFN. Consistent with this finding is that IFN-α4 mRNA levels were upregulated by the two mutants but not the wild-type strain.

The levels of IRF-3, IRF-7, and actin mRNAs decreased about 12 h after infection with the wild-type strain but not the mutant strains (Fig. 5A). This may have been due to the degradation of mRNA by the action of the viral host-shutoff (vhs) protein, which is encoded by the UL41 gene (15). The protein kinase that is encoded by the UL13 gene has also been reported to be involved in the regulation of vhs activity (26).

DISCUSSION

We previously reported that HSV-1 infection leads to inhibition of the IFN signal transduction pathway, as we observed marked suppression of IFN-induced phosphorylation of Jak1, Tyk2, Jak2, STAT1, and STAT2 (44). These results indicate that HSV-1 inhibits the JAK/STAT pathway at a point that precedes the JAK phosphorylation step. In the present study, we showed that SOCS3, a host JAK/STAT inhibitor, is transcriptionally induced by HSV-1 infection. SOCS3 inhibits JAK phosphorylation through binding to the cytokine receptors (3, 14). To our knowledge, only one report showing that virus induces SOCS3 has been published to date. Namely, Bode et al. (4) demonstrated that human hepatitis C virus core protein transcriptionally induces SOCS3, which suppresses the IFN-induced antiviral state. In the case of HSV-1 infection studied here, maximal protein levels of SOCS3 were detected a few hours after virus infection. This finding is consistent with the kinetics of the HSV-1-mediated IFN signal transduction suppression described previously (44). It has been shown that HSV-1 activates IFN-inducible genes under experimental conditions in which de novo cellular protein synthesis was inhibited (23, 24). These observations are consistent with our finding that SOCS3 is synthesized de novo following HSV-1 infection. In addition, UV-treated VR3 did not induce SOCS3, which correlates with its poor inhibition of the JAK/STAT pathway (44). In the previous report, we initially speculated that the virus-mediated inhibition of the JAK/STAT pathway requires viral protein synthesis. However, we found that SOCS3 induction occurs too rapidly (within 10 min) at the mRNA level for it to be driven by the de novo synthesis of viral proteins. Two mutant viruses that are defective in one of the tegument proteins UL41 and UL13, which are hypersensitive to IFN (37, 39), weakly induced SOCS3 compared to the parental wild-type strain. Accordingly, we now postulate that the induction of SOCS3 occurs after endocytosis or uncoating but not at the step of virus attachment to host cells. The UL41 gene product is an RNase, the vhs protein, which rapidly degrades host and virus mRNA and thereby causes protein synthesis shutoff (15). The UL13 gene encodes a protein kinase whose exact function is currently unknown. However, it is proposed that the protein kinase regulates vhs activity (26). The impairment of SOCS3 induction by these mutants should contribute to their hypersensitivity to IFN. However, we found that the mutant viruses are still able to weakly induce SOCS3. Consequently, we propose that the two tegument proteins do not contribute directly to SOCS3 induction. The poor induction of SOCS3 by these mutants may instead relate to the fact that they replicate with a lower efficacy (about 1 log unit less of virus titer) than the parental virus (data not shown).

We also suggest that the induction of SOCS3 by HSV-1 blocks the IFN production system. The IFN production system has been well characterized (5, 18, 31). Initially, IFN-β is transcriptionally activated by phosphorylated IRF-3 and activated NF-κB in a JAK/STAT pathway-independent manner. Virus-induced IFN-β then stimulates the expression of IRF-7, a component of the transactivator of IFN-α genes, via the JAK/STAT pathway (5, 18, 31). IRF-7 subsequently mediates the induction of IFN-α, such as human IFN-α4, and various IFN-inducible genes. This cycle results in the production of large amounts of IFN-α and the establishment of a strong antiviral state. SOCS3, which is induced by HSV-1, may suppress the JAK/STAT-dependent production of large amounts of IFN-α. We found that after HSV-1 infection, IFN-β is upregulated but IRF-7 and IFN-α4 levels are poorly induced (Fig. 5). However, HSV-1 activates IFN- (namely JAK/STAT pathway-) independent signal transduction, including IRF-3 phosphorylation and upregulation of IFN-β (27; also this study). These events were equally well induced by the wild-type virus, VR3, and the mutant viruses d41 and d13. In contrast, the IFN-dependent signal transduction activated by IFN-β is markedly suppressed after infection with VR3 but only partially blocked by infection with the mutant virus particles.

SOCS3 is an important regulator of cytokine signaling. SOCS3 induction would influence not only the IFN system but would also have a dramatic impact on the immune system in a manner that would favor HSV-1 replication. For example, SOCS3 promotes Th2 development by inhibiting interleukin-12 (IL-12)-mediated STAT4 activation in T cells (34). It also negatively regulates IL-2 signaling (6) and IL-2 production via CD28 signaling (19). Furthermore, it inhibits IL-6 signaling in macrophages (8, 16, 40). These SOCS3-mediated events would suppress the ability of the host to clear the virus. We conclude that the induction of SOCS3 by the virus plays a key role in host-virus interactions, as it may directly promote an active and productive infection by the virus. We are currently elucidating the details of the molecular mechanism by which SOCS3 is induced and the effects that it has on both the virus and the host.

ACKNOWLEDGMENTS

This work was supported in part by a Grant-in-Aid for Scientific Research from the Japan Society for the Promotion of Science and by a grant from the Akiyama Foundation.

REFERENCES

1. **Aaronson, D. S., and C. M. Horvath.** 2002. A road map for those who don't know JAK-STAT. Science **296**:1653–1655.
2. **Alcami, A., and U. H. Koszinowski.** 2000. Viral mechanisms of immune evasion. Immunol. Today **21**:447–455.
3. **Alexander, W. S.** 2002. Suppressors of cytokine signalling (SOCS) in the immune system. Nat. Rev. Immunol. **2**:410–416.
4. **Bode, J. G., S. Ludwig, C. Ehrhardt, U. Albrecht, A. Erhardt, F. Schaper, P. C. Heinrich, and D. Haussinger.** 2003. IFN-α antagonistic activity of HCV core protein involves induction of suppressor of cytokine signaling-3. FASEB J. **17**:488–490.
5. **Braganca, J., and A. Civas.** 1998. Type I interferon gene expression: differential expression of IFN-A genes induced by viruses and double-stranded RNA. Biochimie **80**:673–687.
6. **Cohney, S. J., D. Sanden, N. A. Cacalano, A. Yoshimura, A. Mui, T. S. Migone, and J. A. Johnston.** 1999. SOCS-3 is tyrosine phosphorylated in response to interleukin-2 and suppresses STAT5 phosphorylation and lymphocyte proliferation. Mol. Cell. Biol. **19**:4980–4988.
7. **Cooney, R. N.** 2002. Suppressors of cytokine signaling (SOCS): inhibitors of the JAK/STAT pathway. Shock **17**:83–90.
8. **Croker, B. A., D. L. Krebs, J. G. Zhang, S. Wormald, T. A. Willson, E. G. Stanley, L. Robb, C. J. Greenhalgh, I. Forster, B. E. Clausen, N. A. Nicola, D. Metcalf, D. J. Hilton, A. W. Roberts, and W. S. Alexander.** 2003. SOCS3 negatively regulates IL-6 signaling *in vivo*. Nat. Immunol. **4**:540–545.
9. **Darnell, J. E., Jr., I. M. Kerr, and G. R. Stark.** 1994. Jak-STAT pathways and transcriptional activation in response to IFNs and other extracellular signaling proteins. Science **264**:1415–1421.
10. **Fujii, N.** 1994. 2–5A and virus infection. Prog. Mol. Subcell. Biol. **14**:150–175.
11. **Garcia-Sastre, A.** 2001. Inhibition of interferon-mediated antiviral responses by influenza A viruses and other negative-strand RNA viruses. Virology **279**:375–384.
12. **Goodbourn, S., L. Didcock, and R. E. Randall.** 2000. Interferons: cell signalling, immune modulation, antiviral response and virus countermeasures. J. Gen. Virol. **81**:2341–2364.
13. **Gotoh, B., T. Komatsu, K. Takeuchi, and J. Yokoo.** 2002. Paramyxovirus strategies for evading the interferon response. Rev. Med. Virol. **12**:337–357.
14. **Krebs, D. L., and D. J. Hilton.** 2001. SOCS proteins: negative regulators of cytokine signaling. Stem Cells **19**:378–387.
15. **Kwong, A. D., and N. Frenkel.** 1989. The herpes simplex virus virion host shutoff function. J. Virol. **63**:4834–4839.
16. **Lang, R., A. L. Pauleau, E. Parganas, Y. Takahashi, J. Mages, J. N. Ihle, R. Rutschman, and P. J. Murray.** 2003. SOCS3 regulates the plasticity of gp130 signaling. Nat. Immunol. **4**:546–550.
17. **Leonard, W. J., and J. J. O'Shea.** 1998. Jaks and STATs: biological implications. Annu. Rev. Immunol. **16**:293–322.
18. **Mamane, Y., C. Heylbroeck, P. Genin, M. Algarte, M. J. Servant, C. LePage, C. DeLuca, H. Kwon, R. Lin, and J. Hiscott.** 1999. Interferon regulatory factors: the next generation. Gene **237**:1–14.
19. **Matsumoto, A., Y. Seki, R. Watanabe, K. Hayashi, J. A. Johnston, Y. Harada, R. Abe, A. Yoshimura, and M. Kubo.** 2003. A role of suppressor of cytokine signaling 3 (SOCS3/CIS3/SSI3) in CD28-mediated interleukin 2 production. J. Exp. Med. **197**:425–436.
20. **Miller, D. M., B. M. Rahill, J. M. Boss, M. D. Lairmore, J. E. Durbin, J. W. Waldman, and D. D. Sedmak.** 1998. Human cytomegalovirus inhibits major histocompatibility complex class II expression by disruption of the Jak/Stat pathway. J. Exp. Med. **187**:675–683.
21. **Miller, D. M., Y. Zhang, B. M. Rahill, W. J. Waldman, and D. D. Sedmak.** 1999. Human cytomegalovirus inhibits IFN-α-stimulated antiviral and immunoregulatory responses by blocking multiple levels of IFN-α signal transduction. J. Immunol. **162**:6107–6113.
22. **Mossman, K. L.** 2002. Activation and inhibition of virus and interferon: the herpesvirus story. Viral Immunol. **15**:3–15.
23. **Mossman, K. L., P. F. Macgregor, J. J. Rozmus, A. B. Goryachev, A. M. Edwards, and J. R. Smiley.** 2001. Herpes simplex virus triggers and then disarms a host antiviral response. J. Virol. **75**:750–758.
24. **Nicholl, M. J., L. H. Robinson, and C. M. Preston.** 2000. Activation of cellular interferon-responsive genes after infection of human cells with herpes simplex virus type 1. J. Gen. Virol. **81**:2215–2218.
25. **O'Shea, J. J., M. Gadina, and R. D. Schreiber.** 2002. Cytokine signaling in 2002: new surprises in the Jak/Stat pathway. Cell **109**(Suppl.):S121–S131.
26. **Overton, H., D. McMillan, L. Hope, and P. Wong-Kai-In.** 1994. Production of host shutoff-defective mutants of herpes simplex virus type 1 by inactivation of the UL13 gene. Virology **202**:97–106.
27. **Preston, C. M., A. N. Harman, and M. J. Nicholl.** 2001. Activation of interferon response factor-3 in human cells infected with herpes simplex virus type 1 or human cytomegalovirus. J. Virol. **75**:8909–8916.
28. **Remoli, M. E., E. Giacomini, G. Lutfalla, E. Dondi, G. Orefici, A. Battistini, G. Uze, S. Pellegrini, and E. M. Coccia.** 2002. Selective expression of type I IFN genes in human dendritic cells infected with *Mycobacterium tuberculosis*. J. Immunol. **169**:366–374.
29. **Sakai, I., K. Takeuchi, H. Yamauchi, H. Narumi, and S. Fujita.** 2002. Constitutive expression of SOCS3 confers resistance to IFN-α in chronic myelogenous leukemia cells. Blood **100**:2926–2931.
30. **Samuel, C. E.** 2001. Antiviral actions of interferons. Clin. Microbiol. Rev. **14**:778–809.
31. **Sato, M., H. Suemori, N. Hata, M. Asagiri, K. Ogasawara, K. Nakao, T. Nakaya, M. Katsuki, S. Noguchi, N. Tanaka, and T. Taniguchi.** 2000. Distinct and essential roles of transcription factors IRF-3 and IRF-7 in response to viruses for IFN-α/β gene induction. Immunity **13**:539–548.
32. **Schafer, S. L., R. Lin, P. A. Moore, J. Hiscott, and P. M. Pitha.** 1998. Regulation of type I interferon gene expression by interferon regulatory factor-3. J. Biol. Chem. **273**:2714–2720.
33. **Schuringa, J. J., A. T. Wierenga, W. Kruijer, and E. Vellenga.** 2000. Constitutive Stat3, Tyr705, and Ser727 phosphorylation in acute myeloid leukemia cells caused by the autocrine secretion of interleukin-6. Blood **95**:3765–3770.
34. **Seki, Y., H. Inoue, N. Nagata, K. Hayashi, S. Fukuyama, K. Matsumoto, O. Komine, S. Hamano, K. Himeno, K. Inagaki-Ohara, N. Cacalano, A. O'Garra, T. Oshida, H. Saito, J. A. Johnston, A. Yoshimura, and M. Kubo.** 2003. SOCS-3 regulates onset and maintenance of T_H2-mediated allergic responses. Nat. Med. **9**:1047–1054.
35. **Sen, G. C., and R. M. Ransohoff.** 1993. Interferon-induced antiviral actions and their regulation. Adv. Virus Res. **42**:57–102.
36. **Shen, X., F. Hong, V. A. Nguyen, and B. Gao.** 2000. IL-10 attenuates IFN-α-activated STAT1 in the liver: involvement of SOCS2 and SOCS3. FEBS Lett. **480**:132–136.
37. **Shibaki, T., T. Suzutani, I. Yoshida, M. Ogasawara, and M. Azuma.** 2001. Participation of type I interferon in the decreased virulence of the UL13 gene-deleted mutant of herpes simplex virus type 1. J. Interferon Cytokine Res. **21**:279–285.
38. **Song, M. M., K. Shuai, and J. Liao.** 1998. The suppressor of cytokine signaling (SOCS) 1 and SOCS3 but not SOCS2 proteins inhibit interferon-mediated antiviral and antiproliferative activities enhancement of antiproliferative activity of gamma interferon by the specific inhibition of tyrosine dephosphorylation of Stat1. J. Biol. Chem. **273**:35056–35062.
39. **Suzutani, T., M. Nagamine, T. Shibaki, M. Ogasawara, I. Yoshida, T. Daikoku, Y. Nishiyama, and M. Azuma.** 2000. The role of the UL41 gene of herpes simplex virus type 1 in evasion of non-specific host defence mechanisms during primary infection. J. Gen. Virol. **81**:1763–1771.
40. **Yasukawa, H., M. Ohishi, H. Mori, M. Murakami, T. Chinen, D. Aki, T. Hanada, K. Takeda, S. Akira, M. Hoshijima, T. Hirano, K. R. Chien, and A. Yoshimura.** 2003. IL-6 induces an anti-inflammatory response in the absence of SOCS3 in macrophages. Nat. Immunol. **4**:551–556.
41. **Yasukawa, H., A. Sasaki, and A. Yoshimura.** 2000. Negative regulation of cytokine signaling pathways. Annu. Rev. Immunol. **18**:143–164.
42. **Yokota, S., H. Saito, T. Kubota, N. Yokosawa, K. Amano, and N. Fujii.** 2003. Measles virus suppresses interferon-α signaling pathway: suppression of Jak1 phosphorylation and association of viral accessory proteins, C and V, with interferon-α receptor complex. Virology **306**:135–146.
43. **Yokota, S., H. Yanagi, T. Yura, and H. Kubota.** 1999. Cytosolic chaperonin is up-regulated during cell growth. Preferential expression and binding to tubulin at G_1/S transition through early S phase. J. Biol. Chem. **274**:37070–37078.
44. **Yokota, S., N. Yokosawa, T. Kubota, T. Suzutani, I. Yoshida, S. Miura, K. Jimbow, and N. Fujii.** 2001. Herpes simplex virus type 1 suppresses the interferon signaling pathway by inhibiting phosphorylation of STATs and janus kinases during an early infection stage. Virology **286**:119–124.

JOURNAL OF VIROLOGY, Oct. 2004, p. 10303–10309 Vol. 78, No. 19
0022-538X/04/$08.00+0 DOI: 10.1128/JVI.78.19.10303–10309.2004

Signaling through the Prostaglandin I_2 Receptor IP Protects against Respiratory Syncytial Virus-Induced Illness

Koichi Hashimoto,[1,2] Barney S. Graham,[3] Mark W. Geraci,[4] Garret A. FitzGerald,[5] Karine Egan,[5] Weisong Zhou,[1] Kasia Goleniewska,[1] Jamye F. O'Neal,[1] Jason D. Morrow,[1] Russell K. Durbin,[6] Peter F. Wright,[7] Robert D. Collins,[8] Tatsuo Suzutani,[2] and R. Stokes Peebles, Jr.[1]*

Department of Medicine,[1] Department of Pediatrics,[7] and Department of Pathology,[8] Vanderbilt University School of Medicine, Nashville, Tennessee; Department of Microbiology, Fukushima Medical University, Fukushima, Japan[2]; Vaccine Research Center, National Institute of Allergy and Infectious Diseases, National Institutes of Health, Bethesda, Maryland[3]; Department of Medicine, University of Colorado Health Sciences Center, Denver, Colorado[4]; Departments of Medicine and Pharmacology, University of Pennsylvania, Philadelphia, Pennsylvania[5]; and Department of Pediatrics, Ohio State University, Columbus, Ohio[6]

Received 18 November 2003/Accepted 18 May 2004

The role of prostanoids in modulating respiratory syncytial virus (RSV) infection is unknown. We found that RSV infection in mice increases production of prostaglandin I_2 (PGI_2). Mice that overexpress PGI_2 synthase selectively in bronchial epithelium are protected against RSV-induced weight loss and have decreased peak viral replication and gamma interferon levels in the lung compared to nontransgenic littermates. In contrast, mice deficient in the PGI_2 receptor IP have exacerbated RSV-induced weight loss with delayed viral clearance and increased levels of gamma interferon in the lung compared to wild-type mice. These results suggest that signaling through IP has antiviral effects while protecting against RSV-induced illness and that PGI_2 is a potential therapeutic target in the treatment of RSV.

Respiratory syncytial virus (RSV) is the leading cause of respiratory failure in young children and a significant cause of morbidity and mortality in the elderly and patients receiving bone marrow and solid organ transplants (14). Currently, there is no effective vaccine for RSV, and pharmacologic treatment is far from optimal (23). Passive antibody is available to protect selected high-risk infants from severe disease but is limited by its expense (1). The development of new therapeutic agents and vaccine approaches holds the promise of reducing morbidity and mortality from this important pathogen (14).

The role of prostanoids in modulating RSV infection in vivo is unknown. Recent reports suggest that prostaglandin I_2 (PGI_2) alters the host immune response in murine models of pulmonary allergic inflammation (15, 17, 24). PGI_2 is the most abundant arachidonic acid metabolite in vascular tissues, and endothelial cells are the main producers of this prostanoid (9). The principal PGI_2 receptor is IP, a member of a family of eight prostanoid receptors that have conserved homology in mammals, including mice and humans (3). IP is a G protein-coupled rhodopsin-type receptor that has seven transmembrane domains. Binding of PGI_2 to its receptor activates adenylate cyclase via G_s in a dose-dependent manner, increasing the production of cyclic AMP (4). Northern blot analysis reveals that IP mRNA is expressed to the greatest degree in the thymus, while high levels of IP mRNA expression are also found in the spleen, heart, lung, and neurons in the dorsal root ganglia (18).

We found that FVB background mice that are heterozygous for overexpressing PGI_2 synthase in the lung (PGI_2 synthase OE^+) were protected against RSV-induced illness as defined by weight loss and also had decreased lung peak viral replication and gamma interferon (IFN-γ) production compared to littermate controls (PGI_2 synthase OE^-). In contrast, IP-deficient mice ($IP^{-/-}$) of the C57BL/6 background had exacerbated illness with prolonged viral replication. These results reveal that PGI_2 signaling through IP modulates RSV-induced illness.

MATERIALS AND METHODS

Mice. Pathogen-free 10- to 14-week-old mice were used in all experiments. The PGI_2 synthase OE^+ transgenic mice were developed with a construct consisting of a human SP-C promoter and full-length rat PGI synthase cDNA as described previously (10). The SP-C promoter allows targeted expression to alveolar and airway epithelial cells. Transgenic mice were genotyped by performing PCR on genomic DNA isolated from tails as described previously (10). Each line was propagated as heterozygotes. PGI_2 synthase OE^+ mice were always bred with wild-type FVB/N (Jackson Laboratory, Bar Harbor, Maine) mice to produce the experimental PGI_2 synthase OE^+ mice as well as the PGI_2 synthase OE^- littermates, which were used as controls in all of the experiments. For all of the experiments, F_1 mice were used.

In the experiments measuring the PGI_2 urinary metabolite, and female BALB/c mice were purchased from Charles River Laboratories (Wilmington, Mass.). The $IP^{-/-}$ mice were generated by homologous recombination in embryonic stem (ES) cells and were backcrossed 10 generations to the C57BL/6 genetic background (5). The C57BL/6 control wild-type mice were purchased from Jackson Laboratories. Cages, bedding, food, and water were sterilized prior to use. Room temperature was maintained at 27°C, and a 12-h-on, 12-h-off light cycle was provided. In caring for animals, the investigators adhered to the Guide for the Care and Use of Laboratory Animals prepared by the Committee on Care and Use of Laboratory Animals of the Institute of Laboratory Animal Resources, National Research Council (National Institutes of Health Publication No. 86-23, revised 1985).

Cells and virus. HEp-2 cells were maintained in Eagle's minimal essential medium supplemented with glutamine, amphotericin, gentamicin, penicillin G, and 10% fetal bovine serum. The A2 strain of RSV was provided by Robert Chanock, National Institutes of Health. Master stocks and working stocks of RSV were prepared as previously described (12).

Mouse infection. On day 0, mice were infected with RSV or given mock-infected culture medium intranasally as previously described (12). Briefly, the

* Corresponding author. Mailing address: Center for Lung Research, T-1217 MCN, Vanderbilt University Medical Center, Nashville, TN 37232-2650. Phone: (615) 322-3412. Fax: (615) 343-7448. E-mail: stokes.peebles@vanderbilt.edu.

mice were anesthetized with intramuscular ketamine at 40 μg/g and xylazine at 6 μg/g. When held upright with the neck fully extended, the mice readily inhaled a 100-μl inoculum placed over their nostrils with a micropipette. The murine response to RSV infection varies with the strain of mouse. To achieve similar illness as defined by weight loss in our experiments, we administered 1.2×10^7 PFU to mice of the FVB background, 1.9×10^7 PFU in the experiments with mice of the C57BL/6 background, and 0.7×10^7 PFU in the experiments with mice of the BALB/c background. In our experiments, RSV infection with this procedure causes bronchiolitis (12). Each mouse was weighed daily as a measure of RSV-induced illness. Viral replication was ascertained by plaque assay in HEp-2 cells as previously described (12).

Measurement of 2,3-dinor-6-keto-$PGF_{1\alpha}$ in urine. Mice were placed in metabolic cages, and urine was collected daily. Three mice were placed in each cage, and each data point represents the urinary concentration of 2,3-dinor-6-keto-$PGF_{1\alpha}$ for the urine collected from three mice. Nine mice were infected with RSV, and nine mice were mock infected. A gas chromatographic-mass spectrometric assay was used to measure 2,3-dinor-6-keto-$PGF_{1\alpha}$ as previously described (7).

Quantitation of IFN-γ in lung tissues. The concentration of IFN-γ in lung tissue was measured with a commercially available enzyme-linked immunosorbent assay kit (R&D Systems, Minneapolis, Minn.) according to the manufacturer's protocols. On day 6 after infection, each mouse was sacrificed and the lungs were harvested. The left lung from each mouse was ground with a mortar and pestle and ground glass. The solution of the ground lung and the ground glass was then centrifuged at 1,000 rpm for 10 min. The supernatant was then either frozen for later use or added to precoated wells and incubated for 2 h. Dilutions of recombinant cytokine were included for generation of a standard curve. Peroxidase-labeled anticytokine antibody was added to detect bound cytokine, and the plates were developed by the addition of tetramethylbenzidene substrate. Concentrations of IFN-γ in the lung supernatant were calculated from the standard curve produced. The cytokine level from each lung was measured in duplicate.

RSV-specific antibody titers. Blood was drawn 30 days after infection, and after centrifugation, the serum was retained for measurement of RSV-specific antibodies. For measurement of anti-RSV-specific F antibody titers, purified F protein (the kind gift of Wyeth-Lederle, West Henrietta, N.Y.) was diluted in bicarbonate buffer (pH 9.8), added to 96-well plates (Immulon II; Nunc, Roskilde, Denmark) at 10 μg/well, and incubated overnight at 4°C. The same procedure was used for measurement of anti-RSV-specific G antibody titers. The remainder of the protocol is identical for the measurement of both anti-RSV-specific F and G antibody titers. The next morning, the plate was emptied and blocked with 200 μl of 1% bovine serum albumin (Sigma, St. Louis, Mo.). The plate was then washed four times with phosphate-buffered saline–0.5% Tween 20. The serum was then diluted to either 1:1,000 for the $IP^{-/-}$ and wild-type mice, both of the C57BL/6 background, or 1:4,000 for the PGI_2 synthase OE^+ and nontransgenic PGI_2 synthase OE^- littermate mice, both of the FVB background. One hundred microliters of the diluted serum was added to duplicate coated wells, and the plates were incubated overnight at 4°C. The next morning, the plates were washed five times with phosphate-buffered saline–0.5% Tween 20. After washing, 100 μl of biotinylated anti-mouse immunoglobulin G1 (IgG1) (Zymed Laboratories, South San Francisco, Calif.) was added to each well at a dilution of 1:5,000 and incubated 3 h at 37°C. The plates were washed four times with phosphate-buffered saline–0.5% Tween 20. After washing, 100 μl of streptavidin-peroxidase (Sigma) was added to each well at a dilution of 1:2,000 and incubated 1 h at 37°C. The plates were washed four times with phosphate-buffered saline without Tween 20. One hundred microliters of substrate buffer (azinobis-3-ethylbenzthiazolinesulfonic acid in citrate phosphate buffer) was added to each well. Optical density was measured with a 414-nm filter, and values were calculated from a standard curve.

IFN-α/β functional assay. The mouse fibroblast cell line F114 was plated in 96-well plates. The next day, the ground lung supernatant samples to be assayed for IFN were diluted in medium and added to the wells in a twofold dilution series, alongside medium containing known concentrations of commercially obtained mouse IFN-α/β (Access Biomedical). After 24 h, vesicular stomatitis virus was added to the well (multiplicity of infection, ≈2). Two days after infection, cells were stained with crystal violet, and the IFN-α/β concentration was calculated by comparing the dilution giving 50% protection from cell killing with the standard interferon concentration giving similar protection.

SP-A and SP-D content. The surfactant protein A (SP-A) and SP-D in alveolar lavage fluid were analyzed by Western blot in six mice from each genotype. Samples containing 1 μg of saturated phosphatidylcholine were used for analyses of SP-A. Proteins were separated by sodium dodecyl sulfate (SDS)-polyacrylamide gel electrophoresis (PAGE) in the presence of β-mercaptoethanol. After electrophoresis, SP-A was transferred to nitrocellulose paper (Schleicher and Schnell, Keene, N.H.), and immunoblot analysis was carried out with dilution of 1:5,000 guinea pig anti-mouse SP-A and 1:5,000 rabbit anti-mouse SP-D. Appropriate peroxidase-conjugated secondary antibodies were used at 1:5,000 dilutions. Immunoreactive bands were detected with enhanced chemiluminescence reagents (Amersham, Chicago, Ill.). Protein bands were quantitated by densitometric analyses with Alpha Imager 2000 documentation and analysis software (Alpha Innotech, San Leandro, Calif.). The linearity of the assay was confirmed for the range of 10 to 200 ng of mouse SP-A ($R^2 = 0.95$).

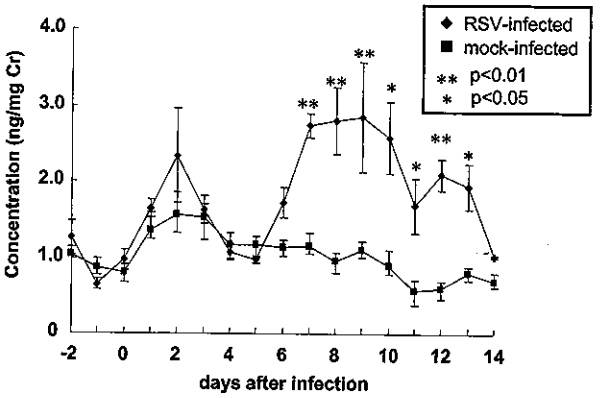

FIG. 1. Concentrations of the PGI_2 metabolite 2,3-dinor-6-keto-$PGF_{1\alpha}$ measured in RSV- and mock-infected BALB/c mice. The data shown are a combination of results from two separate experiments. **, $P < 0.01$ compared to the mock-infected group; *, $P < 0.05$ compared to the mock-infected group.

Protocol for examining lung sections. The mice were sacrificed by cervical dislocation on day 15, and the lung block was removed. The lung tissue was stored in 4% paraformaldehyde, paraffin embedded, cut in 6-μm sections, mounted, and stained with hematoxylin and eosin for routine histology and periodic acid-Schiff to assess mucus. Slides were examined by one observer in a blinded fashion. The following compartments of the lung were assessed: alveolar spaces, airways at all levels, interstitium, and vessels (both arteries and veins). Inflammatory infiltrates were evaluated for location, severity, and composition (cell types: small mononuclear cells, transformed lymphocytes, histiocytes, neutrophils, and eosinophils). The degrees of inflammation were graded as follows: 0, no infiltrate; 1+, most vessels have an infiltrate up to four cells thick; 2+, most vessels have an infiltrate five to seven cells thick; 3+, most vessels have an infiltrate greater than seven cells thick; this score also includes blood or edema fluid in the tissue space.

Statistical analysis. Results are expressed as the mean ± standard error of the mean. Weight curves were analyzed in their entirety by *t* test with analysis of repeated measures. Measurements of viral replication, cytokines, and antibody titers were analyzed by *t* test. Differences were considered significant at $P < 0.05$.

RESULTS

RSV infection increases production of the stable PGI_2 urinary metabolite 2,3-dinor-6-keto-$PGF_{1\alpha}$. We measured the stable PGI_2 metabolite 2,3-dinor-6-keto-$PGF_{1\alpha}$ in the urine of wild-type BALB/c mice that were challenged intranasally with either 0.7×10^7 PFU of RSV (RSV infected) or culture medium (mock infected) to determine if PGI_2 might be involved in the host response to RSV infection. RSV-infected mice had a significant increase in the production of PGI_2 on days 7 to 13 compared to mice challenged intranasally with culture medium (Fig. 1). The increase in the urinary PGI_2 metabolite corresponded to the peak of RSV-induced illness and early recovery phase as defined by weight loss for the FVB (Fig. 2) and C57BL/6 (see Fig. 4) wild-type mice. These results suggest that PGI_2 synthesis is modulated by RSV infection.

Mice that overexpress PGI_2 synthase are protected against RSV-induced illness. Based on the finding that the stable PGI_2

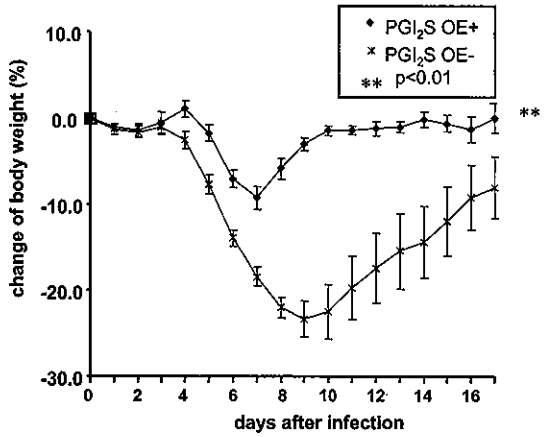

FIG. 2. Daily weight curves of RSV-infected transgenic PGI_2 synthase OE^+ and nontransgenic PGI_2 synthase OE^- littermate control mice, shown as a percentage of the preinfection weight. The data shown are representative of three separate experiments. **, $P < 0.01$ compared to the PGI_2 synthase OE^- mice.

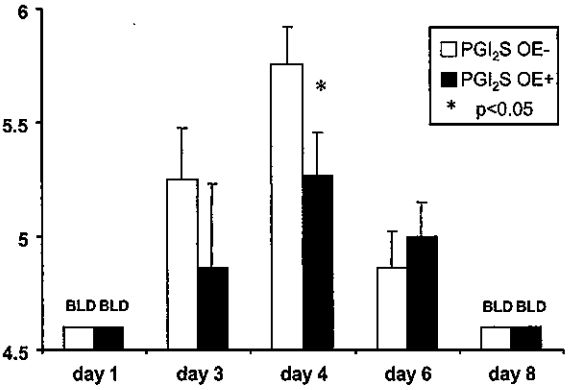

FIG. 3. Viral titers in RSV-infected transgenic PGI_2 synthase OE^+ and nontransgenic PGI_2 synthase OE^- littermate control mice as measured on days 1, 3, 4, 6, and 8 after infection. The viral titers are expressed as $\log_{10}$ PFU per gram of lung tissue. The data shown are representative of three separate experiments. *, $P < 0.05$ compared to the PGI_2 synthase OE^- mice. BLD, below the limit of detection.

urinary metabolite was increased at the peak of infection and during recovery from illness, we hypothesized that PGI_2 was protective against RSV-induced disease. We used transgenic PGI_2 synthase OE^+ and nontransgenic PGI_2 synthase OE^- littermate control mice in our model of RSV infection to test this hypothesis. Consistent high-level expression of PGI_2 synthase was confirmed by increased urinary 2,3-dinor-6-keto-PGF_1 in the PGI_2 synthase OE^+ mice compared to nontransgenic littermate mice (8.11 versus 1.30 ng/mg of creatinine). The PGI_2 synthase OE^+ mice were significantly protected against RSV-induced illness compared to nontransgenic littermates as defined by weight loss ($P < 0.01$) (Fig. 2).

Our group has previously found that illness score correlates with weight loss (12). We found that the peak weight loss in the PGI_2 synthase OE^+ mice was approximately 10% of the preinfection weight, compared to 30% weight loss in the nontransgenic littermate controls. Not only were the PGI_2 synthase OE^+ mice protected against RSV-induced weight loss, but these mice also had decreased peak viral replication compared to the PGI_2 synthase OE^- mice (5.27 ± 0.19 versus 5.76 ± 0.16 $\log_{10}$ PFU/g of lung tissue; $P < 0.05$) on day 4 after infection (Fig. 3).

In an attempt to determine the effect of PGI_2 on IFN-γ production, we measured this cytokine in the lung supernatants of the PGI_2 synthase OE^+ and PGI_2 synthase OE^- mice on day 6 after infection, the time of peak IFN-γ production in the lung. There was a significant decrease in IFN-γ levels in the lung supernatants of the PGI_2 synthase OE^+ compared to the PGI_2 synthase OE^- mice (312 ± 63 versus 532 ± 59 pg/ml; $P = 0.02$). These results suggest that the decreased peak viral replication that was mediated by PGI_2 synthase overexpression is not mediated by production of IFN-γ.

Mice that are deficient in IP have exacerbated illness. Since PGI_2 synthase OE^+ mice were protected against RSV-induced illness, we hypothesized that mice lacking the ability to signal through IP would have greater RSV-induced illness compared to wild-type mice that express IP. To test this hypothesis, we infected $IP^{-/-}$ and strain-matched (C57BL/6) wild-type mice with RSV. We found that $IP^{-/-}$ mice had greater weight loss than wild-type mice (Fig. 4). Although there was no difference between the $IP^{-/-}$ and wild-type mice in peak viral replication on day 4 after infection (data not shown), the $IP^{-/-}$ mice had delayed viral clearance with significantly higher lung viral replication on day 6 after infection compared to wild-type mice (5.41 ± 0.20 versus 4.70 ± 0.22 $\log_{10}$ PFU/g of lung tissue; $P = 0.04$), suggesting that the inability to signal through IP created a deficiency in antiviral immunity (Fig. 5). We also found that levels of IFN-γ in the lung supernatants were significantly greater in the $IP^{-/-}$ mice compared to the wild-type mice ($2{,}260 \pm 133$ versus $1{,}799 \pm 38$ pg/ml; $P < 0.01$). These results indicate that the inability to signal through IP exacerbates RSV-induced weight loss, prolongs viral replication, and increases lung IFN-γ levels.

Inverse relationship between anti-RSV antibody titers and RSV-induced illness. Serum was collected on day 30 after infection and IgG1 anti-RSV antibody titers to the RSV F and Ga protein were measured. PGI_2 synthase OE^+ mice had significantly decreased levels of IgG1 antibodies to both RSV F and RSV Ga compared to the PGI_2 synthase OE^- mice (Fig.

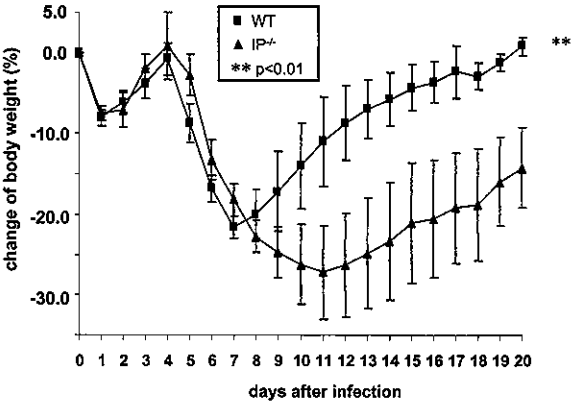

FIG. 4. Daily weight curves of RSV-infected $IP^{-/-}$ and wild-type mice shown as a percent of the preinfection weight. The data shown is representative from two separate experiments. **$P < 0.01$ compared to the wild-type$^-$ mice.

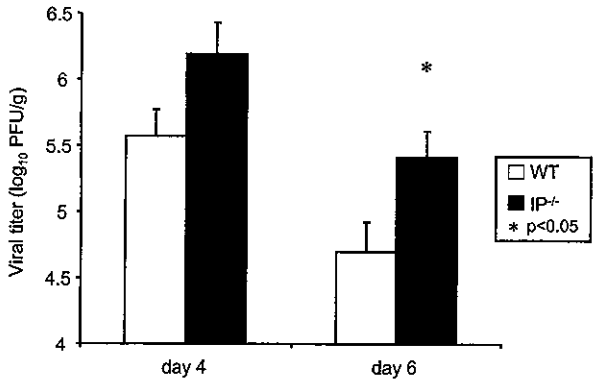

FIG. 5. Viral titers in RSV-infected transgenic $IP^{-/-}$ and wild-type (WT) mice as measured on days 4 and 6 after infection. The viral titers are expressed as log_{10} PFU per gram of lung tissue. The data shown are representative of two separate experiments. **, $P < 0.01$ compared to the wild-type mice.

6), while there was no difference in RSV-specific IgG2a titers between the groups (data not shown). In contrast, there was no statistically significant difference between the anti-RSV IgG1 antibody titers to either RSV F or Ga in the $IP^{-/-}$ and wild-type mice, although there was a trend for an increase in anti-RSV antibody levels in the $IP^{-/-}$ mice. These results suggest that signaling through IP decreases the need for a robust humoral immune response to RSV.

PGI_2 signaling protects against RSV-induced lung edema. Lungs from three mice in each group were harvested on day 8 after infection to examine the inflammatory infiltrate and structural consequences of RSV infection. In both the RSV-infected PGI_2 synthase OE^+ and PGI_2 synthase OE^- groups (Fig. 7), there was 1+ (mild) inflammation consisting primarily of lymphocytosis in the bronchovascular and perivenous spaces. In the lungs of both the PGI_2 synthase OE^+ and PGI_2 synthase OE^- groups, there was focal edema; however, the edema was greater in the PGI_2 synthase OE^- group. There was a similar degree of lymphocytic inflammation in the bronchovascular and perivenous spaces of the lungs of the $IP^{-/-}$ and their wild-type control group, but there was marked widespread edema in the parenchyma of the RSV-infected $IP^{-/-}$ mice that was not present in the lungs of the wild-type mice (Fig. 8). Thus, neither overexpression of PGI_2 synthase nor deficiency in IP had an effect on RSV-induced pulmonary parenchymal lymphocytosis. However, PGI_2 synthase overexpression decreased edema in the lungs of RSV-infected mice of the FVB background, while the inability to signal through IP led to edema in the alveoli in C57BL/6 background mice.

PGI_2 signaling does not affect IFN-α/β production. In order to determine the effect of PGI_2 signaling on RSV-induced IFN-α/β production, we measured IFN-α/β lung activity on day 1 after infection. We found that there was no difference in IFN-α/β lung activity in the PGI_2 synthase OE^+ and PGI_2 synthase OE^- groups (4,310 ± 1,596 versus 4,096 ± 1,122 U/lung, respectively; $n = 5$ for each group). We also found that there was no difference in IFN-α/β lung activity in the $IP^{-/-}$ and wild-type groups (6,554 ± 1,003 versus 4,915 ± 819 U/lung, respectively; $n = 5$ for each group). Therefore, neither overexpression of PGI_2 synthase nor deficiency of IP had an effect on IFN-α/β production 1 day after infection.

PGI_2 synthase overexpression had no effect on SP-A and SP-D production. In order to determine if PGI_2 regulates SP-A

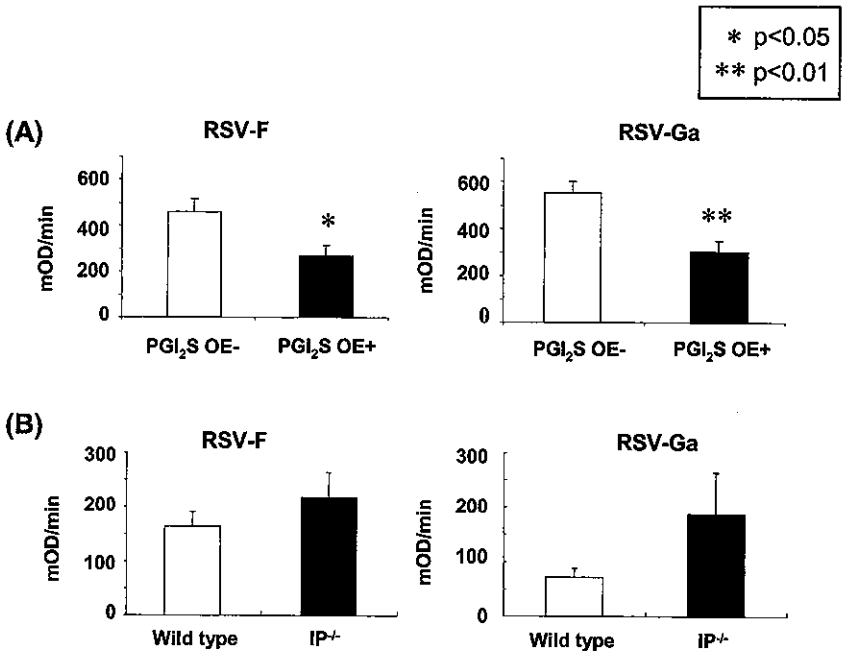

FIG. 6. Measurement of IgG1 anti-RSV antibody titers to the RSV F and Ga proteins on day 30 after infection in PGI_2 synthase OE^+ and PGI_2 synthase OE^- mice as well as in RSV-infected $IP^{-/-}$ and wild-type (WT) mice. **, $P < 0.01$ compared to the PGI_2 synthase OE^- mice; *, $P < 0.05$ compared to the PGI_2 synthase OE^- mice. The data shown are combined from three separate experiments for the PGI_2 synthase OE^+ and PGI_2 synthase OE^- mice and two separate experiments for the $IP^{-/-}$ and wild-type mice.

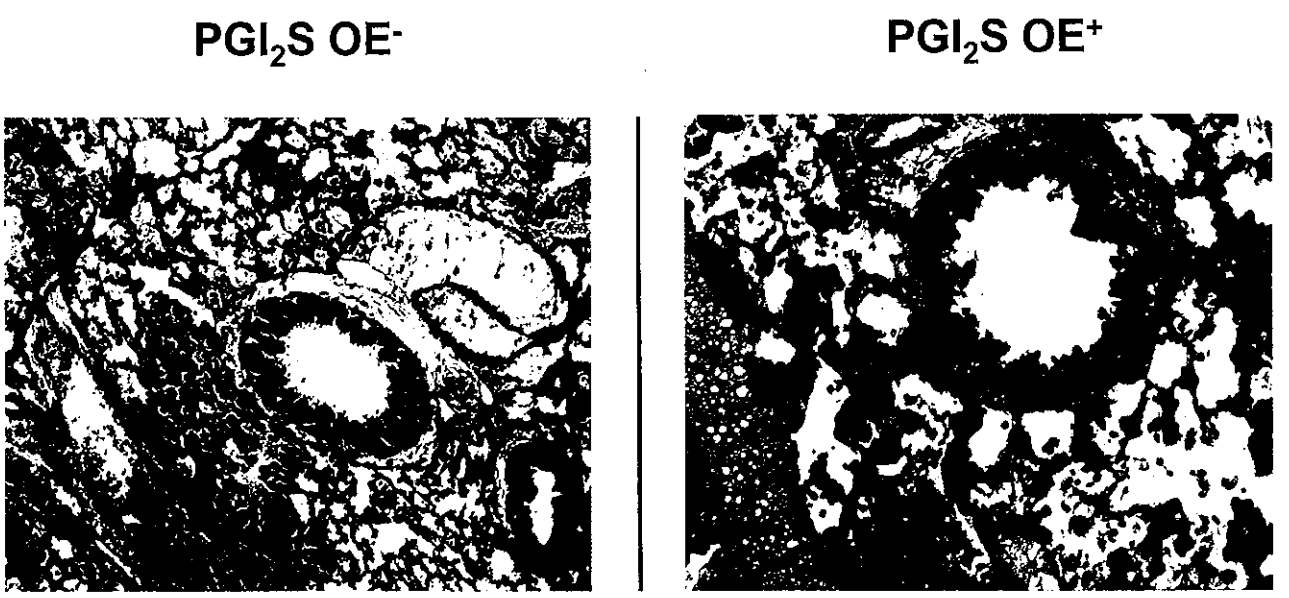

FIG. 7. Lung sections of PGI$_2$ synthase OE$^-$ and PGI$_2$ synthase OE$^+$ mice harvested on day 8 and stained with hematoxylin and eosin. The sections are representative of three mice in each group.

and SP-D production and if such regulation might explain the decrease in peak viral titers in the PGI$_2$ synthase OE$^+$ group, we performed Western blots for surfactant proteins in bronchoalveolar lavage fluid. In uninfected mice, we found no difference in the levels of SP-A and SP-D in bronchoalveolar lavage fluid between the PGI$_2$ synthase OE$^+$ and PGI$_2$ synthase OE$^-$ groups (data not shown, $n = 4$ per group).

DISCUSSION

Our results reveal that PGI$_2$ synthase OE$^+$ mice are protected against RSV-induced illness and have decreased viral replication, while mice that lack IP had exacerbated weight loss and have delayed viral clearance in comparison. These results reveal that PGI$_2$ signaling through IP protects against RSV-induced disease.

We found that production of the stable urinary metabolite of PGI$_2$ is increased by RSV infection. This result is not surprising because a cyclooxygenase enzyme, COX-2, that produces PGI$_2$ is induced as a result of inflammatory stimuli such as tumor necrosis factor alpha that can be generated in the lung as a result of RSV infection (2, 22). However, the expression of the PGI$_2$ metabolite closely corresponds with the period of weight loss that occurs with RSV infection, suggesting that PGI$_2$ may be an important factor in protection from RSV-

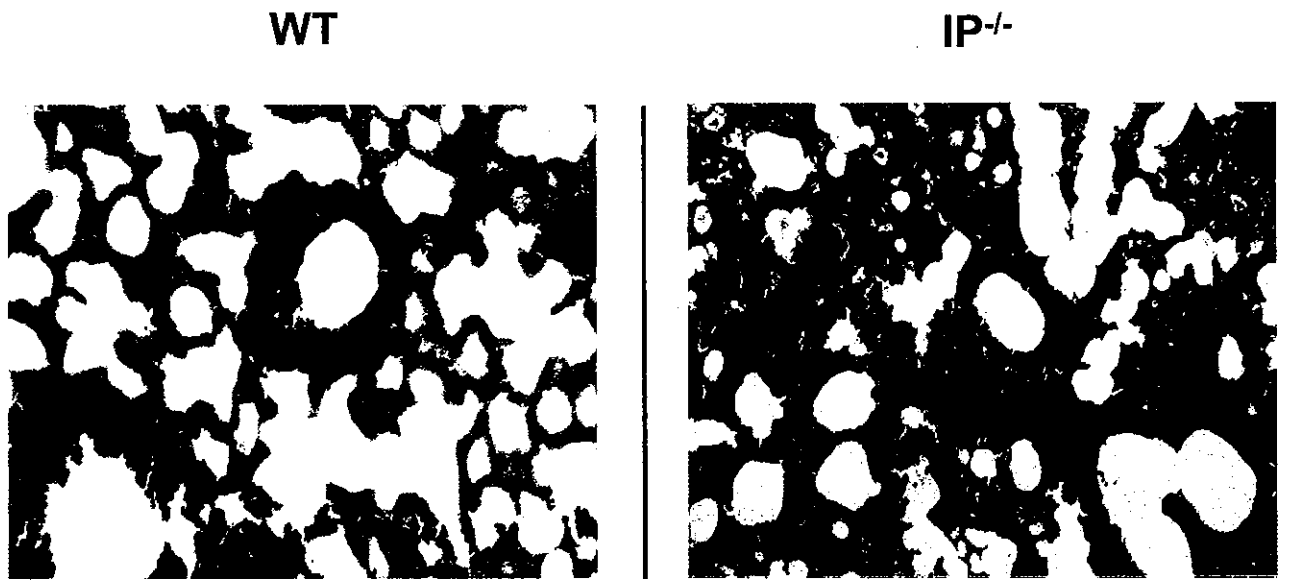

FIG. 8. Lung sections of wild-type (WT) and IP$^{-/-}$ mice harvested on day 8 and stained with hematoxylin and eosin. The sections are representative of three mice in each group.

induced illness. Measures of acute respiratory illness, such as tachypnea, have been noted as early as 1 day after RSV infection (25) and do not correspond to the urinary PGI_2 metabolite that we assayed.

Studies of the murine model of RSV infection reveal that a vigorous adaptive immune response is a key factor in disease severity (11). For instance, when $CD4^+$ and $CD8^+$ lymphocyte subsets are depleted by administration of neutralizing antibody, there is no illness as defined by weight loss or decreased activity, yet RSV replication is prolonged (11). This suggests that the host immune response instead of the viral cytocidal effect is an important determinant of RSV-induced illness. However, we found in our experiments with PGI_2 synthase OE^+ and $IP^{-/-}$ mice and their respective controls that signaling through IP not only protected against weight loss but also decreased viral replication while decreasing IFN-γ production. Given the small yet statistically significant changes in viral titers that occurred in the PGI_2 synthase OE^+ and $IP^{-/-}$ groups in comparison with the respective wild-type mice, it is uncertain whether these changes in viral titers influenced the more dramatic changes seen in weight changes in the groups in response to RSV infection; however, this possibility cannot be ruled out.

Of further note, we found that RSV-specific antibody levels were significantly lower in the PGI_2 synthase OE^+ mice and tended to be higher in the $IP^{-/-}$ mice. The most likely explanation for the decreased IFN-γ levels and anti-RSV antibody titers in the PGI_2 synthase OE^+ mice is an inhibition in peak viral replication in these animals, as a lower antigen load resulted in a decreased need for a robust adaptive immune response to the virus. This suggests that the protective effect of PGI_2 is more likely through cells of the innate immune response, such as NK cells or macrophages.

PGI_2 is known to have a direct effect on NK cells. Iloprost, a PGI_2 analog, increases the NK lytic activity of spleen cells in an ex vivo model of experimental neoplastic metastasis (6). Natural killer cells are activated by both IFN-α and IFN-β (13). PGI_2 affects NK cell function as well as monocyte and macrophage activity. SM-10906, a stable PGI_2 analog, suppressed the production of tumor necrosis factor and interleukin-1 in lipopolysaccharide-stimulated rat pleural resident monocytic cells (19). In addition, PGI_2 regulates the production of tumor necrosis factor alpha in an in vitro assay of murine peritoneal macrophages stimulated with zymosan (21). Carbacyclin, a PGI_2 analog, reduces tumor necrosis factor alpha production from peritoneal macrophages by 50% while increasing the production of interleukin-10 (21).

PGI_2 has only recently been recognized to have immunomodulatory effects in vivo. In murine pulmonary allergen challenge models, mice lacking IP have augmented allergic inflammation as characterized by increases in plasma extravasation, leukocyte accumulation, and type 2 cytokine production in the airway (24). In addition, allergically sensitized $IP^{-/-}$ mice have increased serum antigen-specific IgE and total IgE levels (24). In wild-type mice, PGI_2 production is induced by exposure to an allergen, and IP is expressed by $CD4^+$ type 2 lymphocytes but not by type 1 lymphocytes (24). In vitro, PGI_2 and its stable analog carbaprostacyclin augment interleukin-10 production by $CD4^+$ type 2 cells (15). PGI_2 also has antineoplastic effects. In carcinogenesis models, PGI_2 synthase OE^+ mice have significantly reduced numbers of lung tumors that are proportional to PGI_2 synthase transgene expression (16).

There are only a few reports on PGI_2 in viral infection, but some suggest that PGI_2 may regulate virus-induced illness. For instance, in human immunodeficiency virus-infected patients, the plasma half-life of PGI_2 is diminished to15 to 161 s, compared to 9 to 12 min in noninfected patients; human immunodeficiency virus-infected patients with central nervous system manifestations of their disease have even greater decreases (mean, 34 s) compared to those without such symptoms (mean, 84 s) (20). In lung microvascular endothelial cells from sheep with bluetongue virus infection, PGI_2 is decreased compared to infected endothelial cells from cattle (8). This decrease in PGI_2 production in blue tongue-infected ovine endothelial cells is interesting in that marked pulmonary edema and microvascular thrombosis occur in sheep infected with bluetongue virus but rarely if ever occurs in bluetongue virus-infected cattle (8).

Our histopathology results also suggest that signaling through IP has protective effects against lung edema caused by RSV infection. We found that PGI_2 synthase overexpression decreased edema in the lungs of RSV-infected mice of the FVB background, while the inability to signal through IP led to edema in the alveoli in C57BL/6 background mice. These results suggest that the protective effect of signaling through IP might be a result not only of immunomodulation of RSV infection, but also of preventing vascular leaks leading to lung edema.

In the only prior report investigating the effect of PGI_2 on viral infection in mice, Zavagno and colleagues used a BALB/c mouse model of vaccinia virus infection to investigate the role of the different prostaglandins on illness and viral clearance (26). They found that mice treated with either aspirin or indomethacin, which are cyclooxygenase inhibitors and therefore inhibitors of prostaglandin synthesis, had a marked increase in mortality for vaccinia virus infection over nontreated mice (26). The mice treated with the nonsteroidal anti-inflammatory agents had delayed viral clearance with inhibition of the antibody response, whereas control mice had a higher survival rate with lower virus yield and normal antibody responses. These studies showed that PGD_2 and $PGF_{2\alpha}$ conferred little or no protection to mice against the lethal effects of vaccinia virus, while mice treated with PGE_1 had a dramatic increase in mortality after infection. In contrast, the mice treated with PGI_2 had greatly enhanced survival.

In conclusion, we found that mice overexpressing PGI_2 synthase were protected against RSV-induced weight loss, while mice lacking the PGI_2 receptor IP had exacerbated weight loss after RSV infection. In addition, the mice that overexpressed PGI_2 synthase had decreased peak viral replication, lower lung IFN-γ levels, and lower serum RSV-specific antibody levels, suggesting that PGI_2 overexpression decreased RSV antigen load and downregulated the adaptive immune response. In contrast, $IP^{-/-}$ mice had delayed viral clearance, higher IFN-γ levels in the lung, and slightly increased serum RSV-specific antibody levels, suggesting that the inability to signal through IP increased RSV antigenemia and led to an augmented adaptive immune response.

These results reveal that PGI_2 signaling through its receptor IP protected against RSV-induced illness and decreased viral

replication. Therefore, PGI_2 may be a useful therapy in the prophylaxis of infants at risk for the severe consequences of RSV infection.

ACKNOWLEDGMENTS

This work was supported by an American Academy of Allergy, Asthma and Immunology ERT Award, R01-AI 054660, R01-AI 045512, GM 15431, DK 48831, DK 26657, CA 77839, and Fukushima Medical University.

We thank Jeffrey A. Whitsett and William M. Hull for assistance with the measurement of surfactant protein concentrations and Edith Sanella for measurement of antibody titers.

REFERENCES

1. **American Academy of Pediatrics Committee on Infectious Diseases and Committee of Fetus and Newborn.** 1998. Prevention of respiratory syncytial virus infections: indications for the use of palivizumab and update on the use of RSV-IGIV. Pediatrics **102**:1211–1216.
2. **Aung, S., J. A. Rutigliano, and B. S. Graham.** 2001. Alternative mechanisms of respiratory syncytial virus clearance in perforin knockout mice lead to enhanced disease. J. Virol. **75**:9918–9924.
3. **Breyer, R. M., C. K. Bagdassarian, S. A. Myers, and M. D. Breyer.** 2001. Prostanoid receptors: subtypes and signaling. Annu. Rev. Pharmacol. Toxicol. **41**:661–690.
4. **Breyer, R. M., C. R. Kennedy, Y. Zhang, and M. D. Breyer.** 2000. Structure-function analyses of eicosanoid receptors. Physiologic and therapeutic implications. Ann. N. Y. Acad. Sci. **905**:221–231.
5. **Cheng, Y., S. C. Austin, B. Rocca, B. H. Koller, T. M. Coffman, T. Grosser, J. A. Lawson, and G. A. Fitzgerald.** 2002. Role of prostacyclin in the cardiovascular response to thromboxane A2. Science **296**:539–541.
6. **Costantini, V., A. Giampietri, M. Allegrucci, G. Agnelli, G. G. Nenci, and M. C. Fioretti.** 1991. Mechanisms of the antimetastatic activity of stable prostacyclin analogues: modulation of host immunocompetence. Adv. Prostaglandin Thromboxane Leukot. Res. **21B**:917–920.
7. **Daniel, V. C., T. A. Minton, N. J. Brown, J. H. Nadeau, and J. D. Morrow.** 1994. Simplified assay for the quantification of 2,3-dinor-6-keto-prostaglandin F1 alpha by gas chromatography-mass spectrometry. J. Chromatogr. B Biomed. Appl. **653**:117–122.
8. **DeMaula, C. D., M. A. Jutila, D. W. Wilson, and N. J. MacLachlan.** 2001. Infection kinetics, prostacyclin release and cytokine-mediated modulation of the mechanism of cell death during bluetongue virus infection of cultured ovine and bovine pulmonary artery and lung microvascular endothelial cells. J. Gen. Virol. **82**:787–794.
9. **Galie, N., A. Manes, and A. Branzi.** 2001. Medical therapy of pulmonary hypertension. The prostacyclins. Clin. Chest Med. **22**:529–537.
10. **Geraci, M. W., B. Gao, D. C. Shepherd, M. D. Moore, J. Y. Westcott, K. A. Fagan, L. A. Alger, R. M. Tuder, and N. F. Voelkel.** 1999. Pulmonary prostacyclin synthase overexpression in transgenic mice protects against development of hypoxic pulmonary hypertension. J. Clin. Investig. **103**:1509–1515.
11. **Graham, B. S., L. A. Bunton, P. F. Wright, and D. T. Karzon.** 1991. Role of T lymphocyte subsets in the pathogenesis of primary infection and rechallenge with respiratory syncytial virus in mice. J. Clin. Investig. **88**:1026–1033.
12. **Graham, B. S., M. D. Perkins, P. F. Wright, and D. T. Karzon.** 1988. Primary respiratory syncytial virus infection in mice. J. Med. Virol. **26**:153–162.
13. **Guidotti, L. G., and F. V. Chisari.** 2001. Noncytolytic control of viral infections by the innate and adaptive immune response. Annu. Rev. Immunol. **19**:65–91.
14. **Hall, C. B.** 2001. Respiratory syncytial virus and parainfluenza virus. N. Engl. J. Med. **344**:1917–1928.
15. **Jaffar, Z., K. S. Wan, and K. Roberts.** 2002. A key role for prostaglandin I2 in limiting lung mucosal Th2, but not Th1, responses to inhaled allergen. J. Immunol. **169**:5997–6004.
16. **Keith, R. L., Y. E. Miller, Y. Hoshikawa, M. D. Moore, T. L. Gesell, B. Gao, A. M. Malkinson, H. A. Golpon, R. A. Nemenoff, and M. W. Geraci.** 2002. Manipulation of pulmonary prostacyclin synthase expression prevents murine lung cancer. Cancer Res. **62**:734–740.
17. **Nagao, K., H. Tanaka, M. Komai, T. Masuda, S. Narumiya, and H. Nagai.** 2003. Role of prostaglandin I2 in airway remodeling induced by repeated allergen challenge in mice. Am. J. Respir. Cell Mol. Biol. **29**:314–320.
18. **Narumiya, S., Y. Sugimoto, and F. Ushikubi.** 1999. Prostanoid receptors: structures, properties, and functions. Physiol. Rev. **79**:1193–1226.
19. **Oh-ishi, S., I. Utsunomiya, T. Yamamoto, Y. Komuro, and Y. Hara.** 1996. Effects of prostaglandins and cyclic AMP on cytokine production in rat leukocytes. Eur. J. Pharmacol. **300**:255–259.
20. **Pirich, C., Y. Efthimiou, J. O'Grady, C. Zielinski, and H. Sinzinger.** 1996. Apolipoprotein A and biological half-life of prostaglandin I2 in HIV-1 infection. Thromb. Res. **81**:213–218.
21. **Shinomiya, S., H. Naraba, A. Ueno, I. Utsunomiya, T. Maruyama, S. Ohuchida, F. Ushikubi, K. Yuki, S. Narumiya, Y. Sugimoto, A. Ichikawa, and S. Oh-ishi.** 2001. Regulation of TNFalpha and interleukin-10 production by prostaglandins I(2) and E(2): studies with prostaglandin receptor-deficient mice and prostaglandin E-receptor subtype-selective synthetic agonists. Biochem. Pharmacol. **61**:1153–1160.
22. **Smith, W. L., D. L. Dewitt, and R. M. Garavito.** 2000. Cyclooxygenases: structural, cellular, and molecular biology. Annu. Rev. Biochem. **69**:145–182.
23. **Staat, M. A.** 2002. Respiratory syncytial virus infections in children. Semin. Respir. Infect. **17**:15–20.
24. **Takahashi, Y., S. Tokuoka, T. Masuda, Y. Hirano, M. Nagao, H. Tanaka, N. Inagaki, S. Narumiya, and H. Nagai.** 2002. Augmentation of allergic inflammation in prostanoid IP receptor deficient mice. Br. J. Pharmacol. **137**:315–322.
25. **van Schaik, S. M., N. Obot, G. Enhorning, K. Hintz, K. Gross, G. E. Hancock, A. M. Stack, and R. C. Welliver.** 2000. Role of interferon gamma in the pathogenesis of primary respiratory syncytial virus infection in BALB/c mice. J. Med. Virol. **62**:257–266.
26. **Zavagno, G., B. Jaffe, and M. Esteban.** 1987. Role of prostaglandins and non-steroid anti-inflammatory drugs in the pathogenicity of vaccinia virus. J. Gen. Virol. **68**:593–600.

fections (UTI). Although 11 infants with UTI and aseptic meningitis had no or minimal pyuria, they did have a positive urine culture, which is the standard for diagnosis of UTI. According to the AAP practice parameter regarding diagnosis and treatment of UTI in infants and children, the sensitivity of white blood cells seen on microscopy is only 73% (range, 32 to 100%).[2] The same practice parameter indicates that UTI is likely if a catheterized urine sample grows 10,000 to 100,000 colonies of a single organism, which is the definition of UTI that we used for our study. Results of urine and cerebrospinal fluid (CSF) examinations were included for all infants with UTI and aseptic meningitis so that readers can weigh the evidence for themselves as Dr. Wald has done.

We are not aware of another model of non-central nervous system bacterial infection resulting in a CSF pleocytosis, although case reports of invasive *Yersinia enterocolitica* infections in infants suggest a possible association.[3–5]

Dr. Wald's alternate hypothesis for the association between UTI and aseptic meningitis is interesting. A viral meningitis, perhaps caused by an enterovirus, may be the preceding event in some cases of UTI with aseptic meningitis. However, in our study, aseptic meningitis associated with UTI did not occur more commonly in any particular month or during times of peak enteroviral activity.

Whether a UTI can cause a CSF pleocytosis or a viral meningitis can predispose to a UTI, the major conclusion of our study is that a CSF pleocytosis is not uncommon in young children hospitalized with a UTI and usually does not reflect bacterial meningitis.

Felice C. Adler-Shohet, MD
Jay M. Lieberman, MD
Miller Children's Hospital
University of California, Irvine
Long Beach, California

REFERENCES

1. Adler-Shohet FC, Cheung MM, Hill M, Lieberman JM. Aseptic meningitis in infants younger than six months of age hospitalized with urinary tract infections. *Pediatr Infect Dis J.* 2003;22:1039–1042.
2. American Academy of Pediatrics. Committee on Quality Improvement and subcommittee on Urinary Tract Infection. Practice parameter: the diagnosis, treatment, and evaluation of the initial urinary tract infection in febrile infants and young children. *Pediatrics.* 1999; 103:843–852.
3. Shapiro E. *Yersinia enterocolitica* septicemia in normal infants. *Am J Dis Child.* 1981;135: 477–478.
4. Challapalli M, Cunningham DG. *Yersinia enterocolitica* septicemia in infants younger than three months of age. *Pediatr Infect Dis J.* 1993; 12:168–169.
5. Paisley J, Lauer B. Neonatal *Yersinia enterocolitica* enteritis. *Pediatr Infect Dis J.* 1992;11: 331–332.

Retrospective Diagnosis of Congenital Cytomegalovirus Infection Using Dried Umbilical Cords

To the Editors:

Although blood spots are useful for screening of genetic defects, the materials are not kept long enough or are not always available for retrospective diagnosis of congenital cytomegalovirus (CMV) infection, the major cause of progressive and late onset hearing loss.[1,2] In Japan obstetric hospitals customarily provide dried umbilical cord to every parent as a symbol of the bond between mother and child. Because the embryoblast develops into the umbilical cord and the fetus,[3] we examined whether dried cords might be useful for retrospective diagnosis of congenital CMV infection.

A dried umbilical cord of a 1-year-old boy with congenital CMV infection was obtained from his parents with informed consent. This second child of healthy parents was born at term by cesarean delivery because of fetal distress. Because of tachypnea and spiritlessness the day after delivery, blood and cerebrospinal fluid (CSF) samples were collected. The CSF findings were normal, but elevation of the leukocyte count and serum C-reactive protein indicated some infection; thus he was given antibiotics. Because all symptoms disappeared 8 days later, he was discharged. However, his body weight did not increase well and his extremities gradually became spastic. Brain computed tomography revealed porencephaly and intracranial calcification. Based on detection of CMV genome in the stored CSF (2×10^2 copies/ml), congenital infection was diagnosed.[4] We examined the CMV genome in the dried cords of this case and two healthy 8- and 12-year-old boys by nested PCR (sensitivity limit, 20 copies). Approximately 50 μg of DNA were extracted from 25 mg of the cords. We used 50 ng the DNA for the first round reaction with the primer set that amplifies the entire CMV glycoprotein B gene and 5 μl of the first round products for the second round PCR with the primer set gB1246/gB1604.[5] In the specimen from the case but not from the controls, a single 375-bp fragment was detected, and its CMV sequence was confirmed. The CMV genotype of the case determined by *Hinf* I digestion of the fragment[5] was different from that of the laboratory strain AD169, indicating the PCR specificity.

This is the first report to demonstrate the feasibility of using dried umbilical cords for retrospective diagnosis of congenital CMV infection. Because collection of umbilical cords does not require any extra labor and skill, such as drawing blood and spotting, this assay may provide an alternative approach for epidemiologic studies, including vaccine trials. One concern for the use of umbilical cords is a potential contamination of mother's blood into cords. However, the amount of contaminated blood is relatively small. Furthermore it is unlikely that blood from healthy mothers contains detectable CMV DNA. Actually no CMV DNA was detected in seven additional cords from controls.

This retrospective diagnostic method can be a powerful tool for delineating the exact prevalence of congenital CMV infection in patients with hearing loss from unknown causes.

We thank Risa Takahashi and Felicia R. Stamey for their assistance.

Shin Koyano, MD, PhD
Akiko Araki, MD
Yoshiki Hirano, MD
Kenji Fujieda, MD, PhD
Asahikawa Medical College
Asahikawa, Japan

Tatsuo Suzutani, MD, PhD
Fukusima Medical University School of Medicine
Fukushima, Japan

Kazuyori Yagyu, MD
Obihiro Kyoukai Hospital
Obihiro, Japan

Koichi Murono, MD, PhD
Nayoro City Hospital
Nayoro, Japan

Naoki Inoue, PhD
National Institute of Infectious Diseases
Tokyo, Japan
Centers for Disease Control and Prevention
Atlanta, GA

REFERENCES

1. Fowler KB, McCollister FP, Dahle AJ, Boppana S, Britt WJ, Pass RF. Progressive and fluctuating sensorineural hearing loss in children with asymptomatic congenital cytomegalovirus infection. *J Pediatr.* 1997;130:624–630.
2. Williamson WD, Demmler GJ, Percy AK, Catlin FI. Progressive hearing loss in infants with asymptomatic congenital cytomegalovirus infection. *Pediatrics.* 1992;90:862–866.
3. Benirschke K. The placenta. In: Polin RA, Fox WW, eds. *Fetal and Neonatal Physiology.* 2nd ed. Volume 1. Philadelphia, PA: W. B. Saunders Company; 1998:59–70.
4. Atkins JT, Demmler GJ, Williamson WD, McDonald JM, Istas AS, Buffone GJ. Polymerase chain reaction to detect cytomegalovirus DNA in the cerebrospinal fluid of neonates with congenital infection. *J Infect Dis.* 1994;169:1334–1337.
5. Chou S, Dennison KM. Analysis of interstrain variation in cytomegalovirus glycoprotein B sequences encoding neutralization-related epitopes. *J Infect Dis.* 1991;163:1229–1234.

Monkeypox and Medical Ethics

To the Editors:

In the December 2003 issue, Anderson et al.[1] report a case of human monkeypox from the 2003 US outbreak. They write that many nurses and physicians declined to care for the patient because they had not received smallpox vaccination, whereas others declined "without explanation." They conclude that this case may be "an alarm to the professional community that professional values are changing and that steps need to be taken for professional remediation." We do not believe that this conclusion is supported by the evidence they provide.

Smallpox vaccination is considered to be the most effective prophylaxis available against monkeypox, conferring ~85% protection.[2] Accordingly CDC guidelines recommend that health care workers caring for patients with monkeypox be vaccinated, ideally within the past 1 to 3 years.[2,3] The unvaccinated health care workers who declined to care for the patient therefore acted in accordance with CDC guidelines. In light of this the authors fail to explain why they consider these unvaccinated workers to be in need of professional remediation.

Regarding the health care workers who declined "without explanation," the evidence is also lacking. For instance the authors do not quantitate either the number or the percentage of workers who declined to care for the patient, merely referring to them as 'many.' Also it is not stated whether any of these health care workers had preexisting conditions that might have impacted their decision. For example little is known about the severity of monkeypox infection in persons with HIV infection or other immunocompromised states.[2] In addition, even if the above uncertainties were resolved, it seems tenuous at best to use a single anecdotal case as evidence that the values of an entire profession have changed.

Ultimately the need to assemble a core team to care for the patient is described as an unusual measure and depicted as a regrettable event. In fact the creation of such a team is an appropriate response to cases in which a novel or highly contagious infectious agent is suspected. In October 2002 the Advisory Committee on Immunization Practices recommended that acute care hospitals in the US proactively assemble "Smallpox Healthcare Teams" consisting of vaccinated providers.[4] Such a team would likely have preempted the "unexpected complication" encountered by the authors.

Lastly it is ironic that the authors chose severe acute respiratory syndrome (SARS) as an additional example of an emerging infectious agent. The response to the SARS outbreak has been distinguished by exemplary professional values on the part of innumerable health care workers and scientists around the world.[5] If anything, such a response inspires confidence that professional values in medicine are as strong as they have ever been.

Daniel B. DiGiulio, MD
Paul B. Eckburg, MD
Stanford University School of Medicine
Stanford, California

REFERENCES

1. Anderson MG, Frenkel LD, Homann S, Guffey J. A case of severe monkeypox virus disease in an American child: emerging infections and changing professional values. *Pediatr Infect Dis J.* 2003;22:1093–1096.
2. Di Giulio DB, Eckburg PB. Human monkeypox: an emerging zoonosis. *Lancet Infect Dis.* 2004;4:15–25.
3. Department of Health and Human Services, Centers for Disease Control and Prevention [CDC website]. June 25, 2003. Available at: http://www.cdc.gov/ncidod/monkeypox/treatmentguidelines.htm. Accessed January 22, 2004.
4. Advisory Committee on Immunization Practices [Immunization Action Coalition web site]. October 21, 2002. Available at: www.immunize.org/acip/acip1021. pdf. Accessed January 22, 2004.
5. Gerberding JL. Faster. .. but fast enough? Responding to the epidemic of severe acute respiratory syndrome. *N Engl J Med.* 2003;348:2030–2031.

Acta Neuropathol (2004) 107 : 406–412
DOI 10.1007/s00401-004-0828-0

REGULAR PAPER

Ren-Yong Li · Isao Kosugi · Yoshihiro Tsutsui

Activation of murine cytomegalovirus immediate-early promoter in mouse brain after transplantation of the neural stem cells

Received: 24 September 2003 / Revised: 8 January 2004 / Accepted: 8 January 2004 / Published online: 23 March 2004

Abstract Cytomegalovirus (CMV) is the most significant infectious cause of congenital infection and fatal diseases in immunocompromised patients. We have previously described a transgenic mouse model of the murine CMV (MCMV) immediate-early (IE) gene promoter fused with the lacZ reporter gene (MCMV-IE-pro1) for the analysis of spatiotemporal changes of the promoter activity during brain development. Since expression of the IE genes play a pivotal role in latency and reactivation, we transplanted the transgene-expressing neural stem cells (NSCs) into neonatal mouse brains after labeling with bromodeoxyuridine (BrdU). The activation of MCMV-IE pro1 was detected in the subventricular zone (SVZ) soon after transplantation, and the number of MCMV IE pro1-activated cells was decreased as the development proceeded. Cells that were MCMV IE pro1-activated and glial fibrillary acidic protein positive, but not stained with BrdU, were found in the cortex 4 weeks after transplantation, while BrdU-positive but not MCMV IE pro1-activated cells still existed in the SVZ. MCMV IE promoter activity tended to be easily detected in the cortex after allogenic transplantation in BALB/c mouse. These results suggest that the SVZ is the most susceptible site for activation of the MCMV IE promoter in neonatal mice in the early period after transplantation and that the cerebral cortex is also susceptible to the activation in the late period after transplantation. It may be important to avoid the use of NSCs latently infected with CMV as donor cells.

R.-Y. Li · I. Kosugi · Y. Tsutsui (✉)
Second Department of Pathology,
Hamamatsu University School of Medicine, 1-20-1 Handayama,
431-3192 Hamamatsu, Japan,
Fax: +81-53-4352224,
e-mail: ytsutsui@hama-med.ac.jp

Present address:
R.-Y. Li
Department of Neurophysiology,
Tohoku University School of Medicine, 980-8575 Sendai, Japan

Keywords Cytomegalovirus immediate-early promoter · Neural stem cell · Transplantation · Glial differentiation

Introduction

Cytomegalovirus (CMV), a member of the herpesvirus family, is the most common cause of congenital viral infection in humans [42], with an average incidence of 1% of all live births [33] causing brain anomalies around birth [2, 3, 10] and brain disorders at later times after birth [5, 21]. In adults, infection with human CMV (HCMV) is usually asymptomatic in immunocompetent hosts, but the virus can cause severe or fatal diseases in immunocompromised patients [4]. CMV infection demonstrates a strict host cell type and species specificity [9]. Due to the limitations of studying HCMV in animal hosts, murine CMV (MCMV) infection of mice has been used as a model of HCMV infection with respect to pathogenesis, tissue tropism and latency [17, 32, 38, 39, 40].

Like the genes of HCMV and other herpesviruses, MCMV genes are expressed in three sequential phases: immediate-early (IE), early and late phase [9, 19]. The expression of IE genes is highly dependent on appropriate cellular transcription factors that bind to the DNA sequence of the CMV major IE (MIE) promoter/enhancer [7, 20]. MIE genes are the first to be transcribed [34] and control of viral IE gene expression is believed to play an important role in determining viral replication and latency, which is associated with restricted IE gene expression [12, 15].

Previously, we reported cell type-specific expression of the MCMV IE promoter-lacZ gene in transgenic mice [1]. Astrocyte-specific expression of the transgene was observed in the brains of the transgenic mice. We further showed spatiotemporal changes in the activity of the MCMV IE promoter during mouse brain development [18]. We found that the MCMV IE promoter was predominantly activated in the neural progenitor cells after the differentiation of the neural stem cells (NSCs) from the transgenic mice [18].

In the present study, we identified the sites of the developing brain susceptible to activation of the MCMV IE

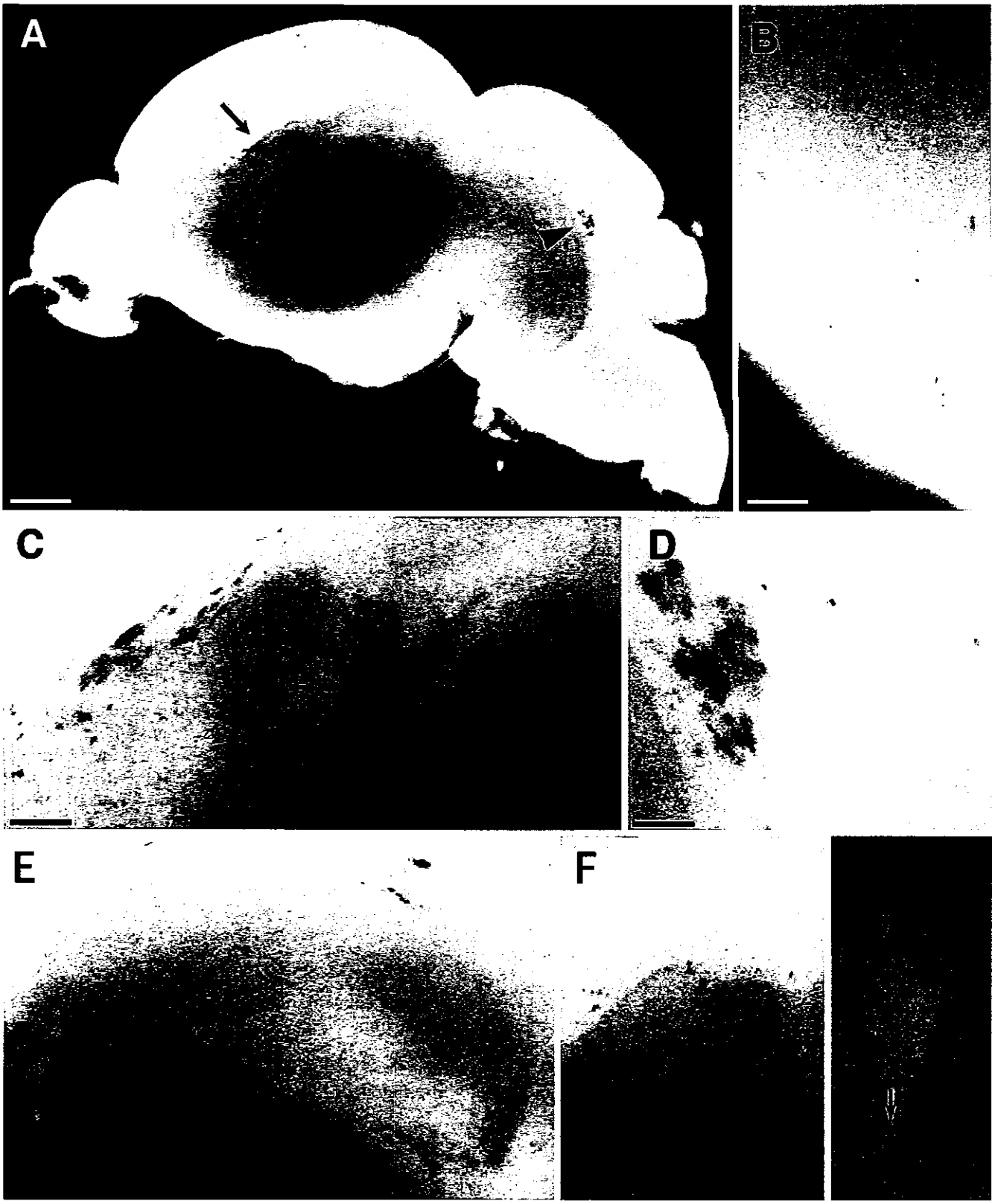

Fig. 1 MCMV IE promoter activity is first detected in the periventricular area after transplantation. Sagittal sections of whole brain (**A–D**) 1 day after transplantation and coronal sections of brain 1 day (**E**), 5 days (**F**), 14 days (**G**) after transplantation. X-Gal-positive cells are detected in lateral ventricle (**A** *arrow*, **C**), fourth ventricle (**A** *arrowhead*, **D**) and cortex(**B**, **E**). Activation of the transgene (**G** *arrows*) decreases in the subventricular zone (**E–G**) with development after transplantation (*CMV* cytomegalovirus, *MCMV IE* murine CMV immediate-early gene). *Bar* **A** 500 μm; **B–G** 100 μm

promoter after transplantation of neural stem cells from the transgenic mice.

Materials and methods

Primary neurosphere cultures

NSCs were cultured as neurospheres according to the method of Reynolds and Weiss [26, 27]. Neurospheres from transgenic embryonic mouse brains, which expressed the lacZ gene under transcriptional control of the MCMV major IE promoter (MCMV-MIE pro1, nucleotides –1,343 to –6) were cultured as described previously [1, 18]. The cerebral cortex was removed on embryonic day 18.5 (E18.5). After mechanical dissociation, single-cell suspensions were grown in a 1:1 mixture of Dulbecco's modified Eagle's medium (DMEM) and F-12 nutrient (Gibco). Cells were plated as 4×10^6 cells/20 ml in 75-cm^2 tissue culture flasks (Falcon) in medium comprising DMEM/F-12 (1:1) containing 5 mM HEPES buffer, 0.6% glucose, 3 mM sodium bicarbonate and 2 mM glutamine, supplemented with following defined mixture of hormones and salt: 25 μg/ml insulin, 100 μg/ml transferrin, 20 nM progesterone, 60 μM putrescine and 30 nM sodium selenite. To the above medium, 20 ng/ml epidermal growth factor (purified from the mouse submaxillary gland; Collaborative Res., Bedford, MA) was added.

Transplantation of the NSCs into neonatal mouse brain

Transplantation of the CNS stem cells was performed basically as described previously [14]. CNS stem cells that had been cultured for 4 days were labeled with 0.5 μM bromodeoxyuridine (BrdU) for 48 h. After dissociation in the presence of 0.001% deoxyribonuclease (Sigma), the stem cells were pelleted and suspended in the growth medium. Newborn mice (within 24 h after birth, C57BL/6 and BALB/c mice) were injected with the stem cells (2×10^5 cells/7 μl) in one side of the cerebral hemisphere using a 10-μl Hamilton syringe with a 27-gauge needle. After transplantation, the neonatal mice were killed on various days. After fixation in 4% paraformaldehyde (PFA) in 0.1 M phosphate buffer (PB) for 2 days at 4°C, coronal slices of the frontal, parietal, occipital and cerebellar parts of the brains were embedded in paraffin and sectioned for immunochemical analysis.

X-Gal staining

Fixation and staining of the brains were performed as previously reported [18]. Brains removed at various times after transplantation were sectioned and fixed in freshly prepared 2% PFA and 0.1% glutaraldehyde (GA) in 0.1 M PB at 4°C for 60–90 min with shaking, rinsed in phosphate-buffered saline (PBS) and washed three times with PBS, then stained at 4°C overnight with shaking in staining solution containing 1 mg/ml 5-bromo-4-chloro-3-indolyl-β-D-galactopyranoside (X-Gal), 5 mM $K_3Fe(CN)_6$, 5 mM $K_4Fe(CN)_6$ $3H_2O$, 2 mM $MgCl_2$, 0.01% sodium deoxycholate and 0.02% Nonidet P-40 in PBS (pH 7.4). The brain sections were postfixed in 4% PFA for 1 h and then photographed and embedded in paraffin for histological examinations.

Immunohistochemical analysis

Postnatal mice were killed under anesthesia with ether and the brains were removed and fixed overnight in 4% PFA in 0.1 M PB at 4°C. After fixation, coronal slices of the frontal, parietal, occipital and cerebellar parts of the brains were embedded in paraffin and sectioned. After deparaffinization and rehydration, sections were pretreated with 0.3% hydrogen peroxide and incubated with goat serum blocking solution for 10 min. The sections were incubated with anti-β-galactosidase antibody (anti-β-Gal;1:1,000 dilution, Cappel, Durham, NC) overnight at 4°C, and then with horseradish peroxidase (HRP)-conjugated goat anti-rabbit IgG, and finally colored with 3-amino-9 ethylcarbazole (AEC; Dako, Tokyo) [1, 18]. For the serial brain sections, sections adjacent to those reacted with X-Gal or stained with anti-β-Gal were incubated with the following primary antibodies (Ab): mouse monoclonal Ab (mAb) to BrdU (1:20, Dako, Denmark); mouse mAb to microtubule-associated protein 2a and 2b (MAP2; 1:100, Sigma, St. Louis, MO) and to neuron-specific enolase (NSE; 1:100, Novocastra Lab., Newcastle, UK) for neurons, rabbit antibody to glial fibrillary acidic protein (GFAP; 1:5, Dako Corp, Carpinteria, CA) or mouse mAb to GFAP (1:100, Sigma) for astrocytes, a rabbit antibody to nestin (1:100, a gift from Dr. H. Kitani, National Institute of Animal Health, Tsukuba, Japan) [37] for undifferentiated neural precursor cells [16], or mouse mAb to myelin-associated glycoprotein (MAG; 1:100, Boehringer Mannheim Biochemica, Mannheim, Germany) for oligodendrocytes. The sections were incubated with biotinylated secondary antibodies and with HRP-conjugated streptavidin, and colored with AEC or with 3,3'-diaminobenzidine [28, 29].

In situ hybridization

To detect the transplanted cells, in situ hybridization was performed as described previously [28]. The probe used in this study was the *Bam*HI fragment (1.3 kb) of the transgene containing the MIE pro1 as described previously [1], with digoxin tail labeling.

Results

MCMV-IE promoter activity was first detected in the subventricular zone after transplantation

We transplanted NSCs (passaged three times) from E18 transgenic mice into newborn mouse brains within 24 h after birth. By 1 day after transplantation, the whole brain was stained with X-Gal (Fig. 1A–E). MCMV MIE pro1-activated cells was observed in the ventricular walls of the lateral ventricle (Fig. 1A, C, E–G), third ventricle (Fig. 1A, C) and fourth ventricle (Fig. 1A, D). Some X-Gal-positive cells were also observed in marginal regions (Fig. 1A, B). X-Gal-positive cells were observed in the ventricular zone (VZ) and subventricular zone (SVZ) 1 day (Fig. 1E), 5 days (Fig. 1F) and 14 days (Fig. 1G) after transplantation.

Transplanted cells migrated to the cerebral cortex and hippocampus

The transplanted cells, which had been labeled with BrdU in vitro, migrated to the cerebral cortex and hippocampus

Fig. 2 Transplanted NSCs migrate to the cerebral cortex (**A–C**) ▶ and hippocampus (**A**, **D**, **E**) 5 days after transplantation. BrdU-positive cells (*blue*) are double-stained with anti-GFAP Ab (**C**, **E**, **G**; *red*) and anti-nestin Ab (**D**; *red*),but hardly stained with anti-NSE Ab (**A**, **B**, **H**; *red*).The number of BrdU-positive cells decreases with development: 1 day (**F**), 5 days (**G**) and 30 days (**H**) after transplantation (*NSC* neural stem cell, *GFAP* glial fibrillary acidic protein, *NSE* neuron-specific enolase, *CP* cortical plate, *IZ* internal zone, *SVZ* subventricular zone, *HI* hippocampus). *Bar* **A** 200 μm; **B–E** 30 μm; **F–H** 100 μm

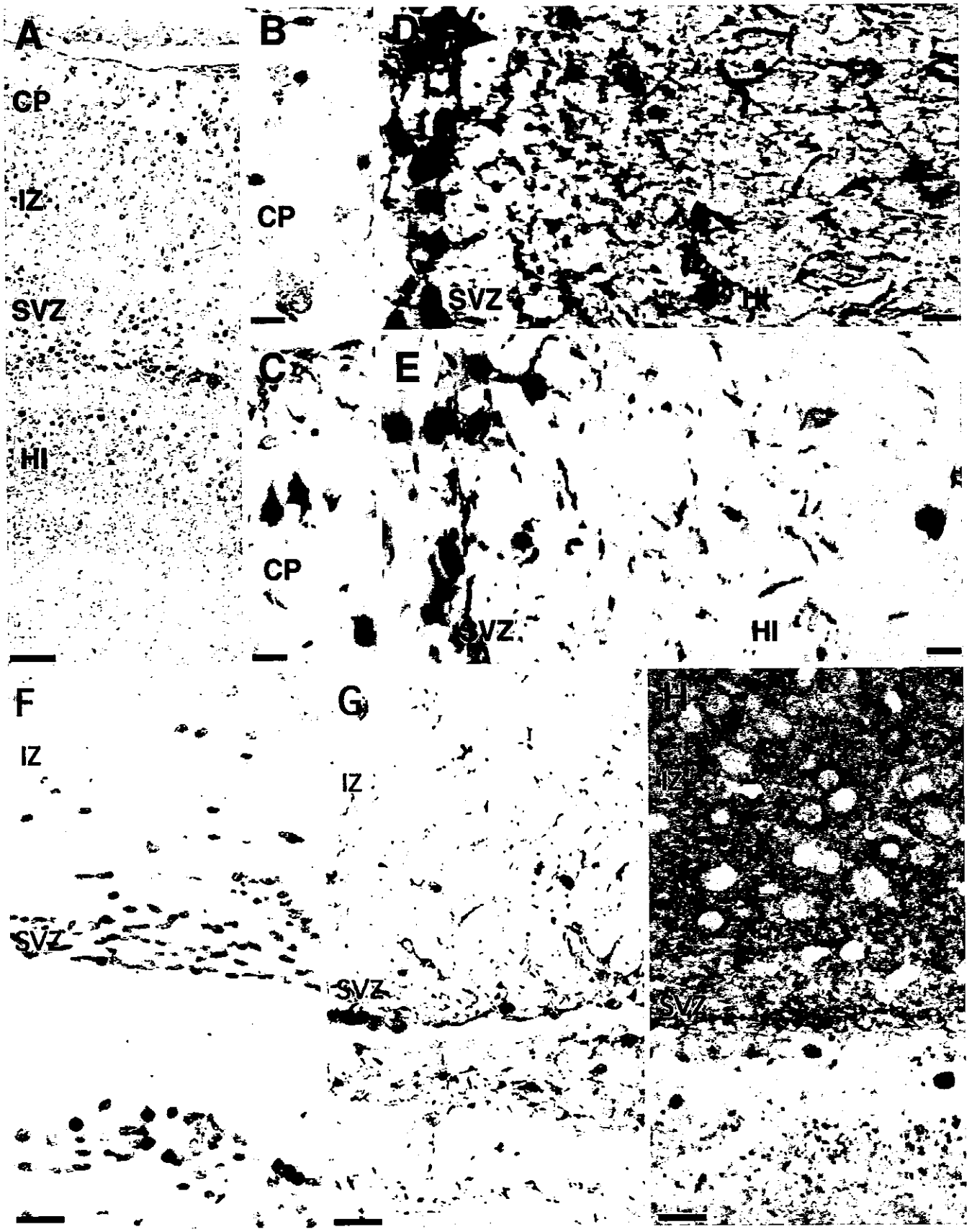
A
CP
IZ
SVZ
HI
B
CP
C
CP
D
SVZ
HI
E
SVZ
HI
F
IZ
SVZ
G
IZ
SVZ
H
IZ
SVZ

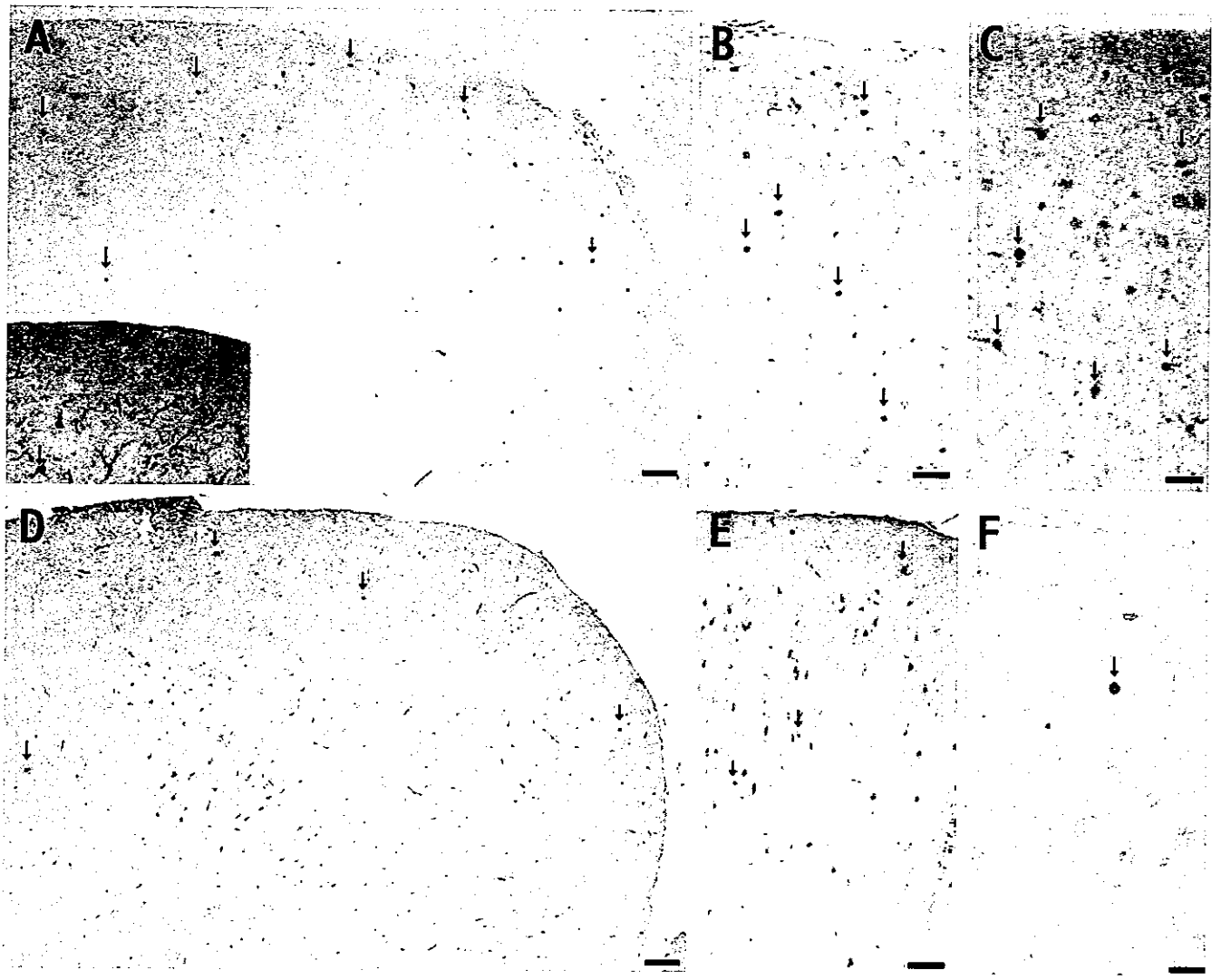

Fig. 3 The transgene in the transplanted NSCs is activated in the cortex in young adult mice. MCMV IE pro1-activated cells are detected in the cortex 30 days after transplantation (**A**, **B**, *arrows*) by immunohistochemical staining with anti-β-Gal Ab. These cells are also double-stained with anti-GFAP Ab (*insert* in **A**, *arrow*). The transgene DNA is detected by in situ hybridization (**D**, **E**). Activation of the MCMV IE pro1 is detected at 14 days after transplantation into BALB/c mice (**C**) but is hardly detected at that time in C57BL/6 mice (**F**). *Bar* **A**, **D** 300 μm; **B**, **C**, **E**, **F** 150 μm

by 5 days after transplantation (Fig. 2A–E, G). Among these BrdU-positive cells, 75% were double-stained with anti-GFAP Ab (Fig. 2C, E, G), 72% with anti-nestin Ab (Fig. 2D), and about 5% with anti-NSE Ab (Fig. 2A, B). These results suggest that most BrdU-positive cells are neural progenitor cells at this stage and may have migrated from the ventricular walls. BrdU-positive cells were observed in the SVZ from day 1 (Fig. 2F), and were retained in the SVZ at 5 days (Fig. 2G) and at 30 days after transplantation (Fig. 2H). Most of these BrdU-labeled cells expressed GFAP (Fig. 2C,E, G), but only a small fraction of the positive cells expressed NSE (Fig. 2A, B, H). However, activation of the IE promoter was not observed in the SVZ at 30 days after transplantation, although the BrdU-positive cells still remained in the SVZ (Fig. 2H).

Activation of the MCMV IE promoter in the cerebral cortex at late times after transplantation

Transgene-expressing cells gradually decreased in the SVZ as development proceeded (Fig. 1E–G). Transgene-expressing cells began to appear in the cerebral cortex from 2 weeks, and the expression was still detected at 30 days after transplantation (Fig. 3A, B). Viral DNA was also detected in the same region by in situ hybridization (Fig. 3D, E). The transgene-expressing cells were double-stained with anti-GFAP Ab (Fig. 3A, insert), but not with anti-NSE Ab (not shown).

Passaged NSCs were activated in cerebral cortex by transplantation into BALB/c mice but hardly activated in C57BL/6 mice

In our previous report [18], MCMV IE promoter activity was shown to decrease as the number of passages in-